

# Intermolecular Potentials from Crystal Data. V. Crystal Packing of Poly[ $\beta$ -(*p*-chlorobenzyl)-L-aspartate]<sup>1</sup>

Yi-Chang Fu,<sup>2a</sup> Robert F. McGuire,<sup>2b</sup> and Harold A. Scheraga\*

Department of Chemistry, Cornell University, Ithaca, New York 14850.

Received January 14, 1974

**ABSTRACT:** Conformational energy calculations were carried out for crystals of poly[ $\beta$ -(*p*-chlorobenzyl)-L-aspartate] (*p*-Cl-PBLA) in both the  $\alpha$ - and  $\omega$ -helical forms, starting both with conformations computed earlier for the isolated homopolymer and with those deduced from X-ray diffraction and infrared dichroism measurements on fibers. The energy of the crystal was minimized with respect to the intramolecular variables (backbone and side-chain dihedral angles), the relative orientation of the helices, and the lattice parameters of the crystal. One component of the entropy (*viz.*, the entropy for variation of the relative orientation of the helices) was computed to show in a simple way how the optimal packing structure in the crystal can be influenced by entropy effects. The orientations of the transition moments of the side-chain chromophores, and the distance of the chlorine atom, with respect to the helix axis were computed and compared to the experimental values from infrared dichroism and X-ray diffraction as a check on the minimum-energy conformation of the crystal. The  $\alpha$ -helical conformation found earlier to be the most stable one for the isolated homopolymer also appears to be the most stable conformation in the crystal. The nonbonded interactions are the primary stabilizing forces, and it appears that reorientation of the side chains in the crystal may distort the backbone conformation slightly to gain additional stability. Electrostatic interactions do not appear to play a major role in influencing the crystal structure. These conformational energy calculations also indicate that a stable  $\omega$ -helical form (with slightly nonplanar peptide bonds) should exist in the crystal. In agreement with earlier calculations on other crystals, the  $\omega$ -helix appears to be stabilized by intermolecular interactions in the crystal. The same type of entropy term gives added stability to both the  $\alpha$ - and  $\omega$ -helix, and tends to improve the agreement between the computed and experimental values.

In a previous paper,<sup>3</sup> we computed the packed crystal structures of two poly(amino acids) with empirical energy functions, using two separate sets of nonbonded parameters for *intra*- and *intermolecular* interactions, respectively. We have subsequently improved the potential functions,<sup>4,5</sup> and apply our earlier procedure<sup>3</sup> to the crystal packing of poly[ $\beta$ -(*p*-chlorobenzyl)-L-aspartate] (*p*-Cl-PBLA), which has been shown<sup>6</sup> by X-ray diffraction to exist in both the right-handed  $\alpha$ - and  $\omega$ -helical forms in fibers. With the improved potential functions,<sup>4,5</sup> we can now treat both *intra*- and *intermolecular* interactions using the same set of parameters. The potential energy of the crystal is minimized, and the minimum-energy polymer conformation, the orientations of the vibrational transition moments in the side chain, and the calculated lattice constants of the crystal are compared with experimental values for both the  $\alpha$ - and  $\omega$ -helical forms of *p*-Cl-PBLA. In the calculation of the lattice constants, we include an approximate entropy for the rotational freedom about the helix axis of the poly(amino acid) within the crystal lattice.

This polymer was selected as an example of the family of esters of poly(aspartic acid) which exhibit interesting properties both from an experimental<sup>6-23</sup> and a theoretical<sup>24-26</sup> point of view. These poly(amino acids) take on various chain conformations both in solution and in fibers depending on the temperature, the solvent, and the intrinsic properties of the different ester side chains. Poly( $\beta$ -methyl-L-aspartate),<sup>12,17</sup> poly( $\beta$ -benzyl-L-aspartate),<sup>7,8</sup> and the *o*- or *m*-chloro-substituted benzyl polymer<sup>19</sup> are known to occur in the left-handed  $\alpha$ -helix conformation, while the polymers obtained by conversion of the methyl to an ethyl, *n*-propyl, isopropyl, or *n*-butyl group,<sup>17</sup> or by substitution of a nitro, chloro, methyl, or a cyano group in the para position of the benzyl group,<sup>14-16</sup> exhibit a reversal of the helix sense (to right handed) of the aspartate polymer. Also, the conformation of poly( $\beta$ -benzyl-L-aspartate) is known to change from a left-handed  $\alpha$  helix in solution<sup>7,8</sup> to a left-handed  $\omega$  helix when it is packed into crystals (stretched fibers and films<sup>27,28</sup>). Finally, *p*-Cl-PBLA exists as a right-handed  $\alpha$  helix in solution<sup>16</sup> but as

a right-handed  $\alpha$  or  $\omega$  helix in fibers.<sup>6</sup> Since molecules in fibers would be less perturbed by solvent molecules than are individual molecules in solution, the  $\alpha$  and  $\omega$  forms of *p*-Cl-PBLA were selected for an application of the improved potential functions<sup>4,5</sup> to packed crystal structures.

## Theory

**A. Geometry.** The bond lengths and bond angles<sup>5</sup> shown in Figure 1 were held fixed in all these calculations.<sup>29</sup> The conformation of the homopolymer was altered by variation of the backbone dihedral angles<sup>31</sup>  $\phi$ ,  $\psi$ ,  $\omega$  and the side-chain dihedral angles<sup>31</sup>  $\chi_i$  ( $i = 1-5$ , as in Figure 2), and this set of angles was held fixed in every residue (regularity condition).

As before,<sup>3</sup> using the same coordinate transformations, the helix structure was generated from the coordinates of one residue. The helix backbone was defined in terms of  $\omega$ ,  $t$ , and  $h$  (which are related to  $\phi$  and  $\psi$  by the Sugeta-Miyazawa equations<sup>32</sup>), where  $t$  is the angle of rotation around the helix axis from the origin of one residue to the origin of the succeeding residue, and  $h$  is the corresponding translation along the helix axis.

In order to position this regular homopolymer in the unit cell to form the observed<sup>6,29</sup> crystal lattice (hexagonal for the  $\alpha$  helix and tetragonal for the  $\omega$  helix) of *p*-Cl-PBLA, a helix coordinate system is assigned to the reference chain as follows. The origin of this coordinate system is chosen so that the *i*th C $\alpha$  atom lies on the positive  $x$  axis which is perpendicular to the helix axis and the  $z$  axis is coincident with the helix axis (taken positive from the N to C terminus), with the  $y$  axis taken to complete a right-handed orthogonal coordinate system. The remainder of the atoms in this chain are then determined using eq 22 and 25 of ref 32. This reference chain is then positioned within the unit cell by aligning the  $z$  axis of the molecule to coincide with the  $c$  axis of the crystal, with the origin of the coordinate system on the reference molecule placed so that the  $x$  axis is initially coincident with the  $a$  axis of the unit cell. This molecule may then be translated in the positive  $c$  direction by  $\Delta z$  and the  $x$  axis rotated about the  $c$  axis by an amount  $z_{\text{rot}}$ , the positive

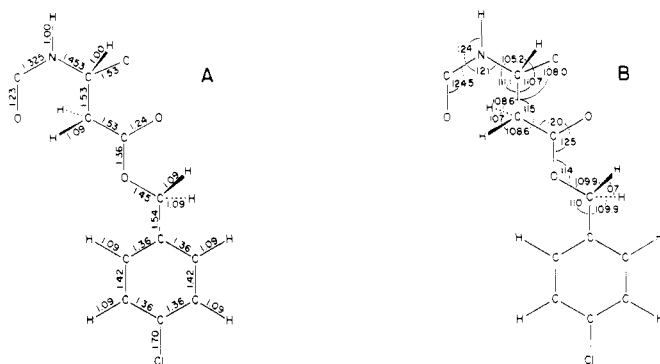


**Figure 1.** Bond lengths in Ångstrom units (A) and bond angles in degrees (B) of the  $\beta$ -(*p*-chlorobenzyl)-L-aspartate residue. In (B), all bond angles of the aromatic group are  $120^\circ$ .

direction of rotation being the right-handed one when looking from the N to the C terminus. Additional molecules are then placed in the unit cell and additional unit cells constructed by using symmetry operations on this reference molecule. See McGuire *et al.*<sup>3</sup> for a more complete description of these procedures and the equations for the transformation of coordinates, generation of the helical structure, and the symmetry operators used to generate molecules within the unit cell and to generate additional cells.

**B. Energies.** The total potential energy of the crystal, reported as energy per residue, is the sum of all *intramolecular* interactions, which include torsional, nonbonded, hydrogen-bond, and electrostatic interactions *within* a molecule, plus the *intermolecular* interactions, which include nonbonded, hydrogen bond and electrostatic interactions *between* molecules within the crystal structure. The calculation of energies was carried out so that all pairwise interactions within a  $3 \times 3 \times 3$  crystal lattice were included.<sup>3</sup>

For all nonbonded interactions between atoms *i* and *j*, the following form of the Lennard-Jones 6-12 potential was used:

$$U_{nb}(r_{ij}) = \epsilon_{ij}[(\langle r \rangle_{ij} / r_{ij})^{12} - 2.0(\langle r \rangle_{ij} / r_{ij})^6] \quad (1)$$

where  $r_{ij}$  is the interatomic distance,  $\langle r \rangle_{ij}$  is the distance for which the nonbonded energy of the *ij* pair is a minimum, and  $\epsilon_{ij}$  is the depth of the potential well at  $\langle r \rangle_{ij}$ . The parameters  $\langle r \rangle_{ij}$  and  $\epsilon_{ij}$  were taken from Momany *et al.*,<sup>5</sup> who derived this set from the best fit to the crystal structures of a series of small molecules. This set of parameters is used here for both the *intra*- and *intermolecular* interactions. For the *intramolecular* nonbonded interactions, only interactions between pairs of atoms separated by three or more bonds were included, except in those cases in which the interatomic distance remained constant because the corresponding groups were not permitted to rotate (e.g., in a ring).

The empirical general hydrogen-bond potential of McGuire *et al.*<sup>4</sup>

$$U_{GHB} = A/r_{O \cdots H}^{12} - B/r_{O \cdots H}^{10} \quad (2)$$

was used to treat hydrogen bonds, where *A* and *B* are the specific parameters for a  $C=O \cdots H-N$ -type hydrogen bond, and  $r_{O \cdots H}$  is the distance between the specific O and H atoms in question.

All electrostatic interactions were calculated between nonbonded atom pairs (atoms separated by three or more bonds except in those cases in which the interatomic distance remained constant because the corresponding groups were not permitted to rotate) using the coulombic potential

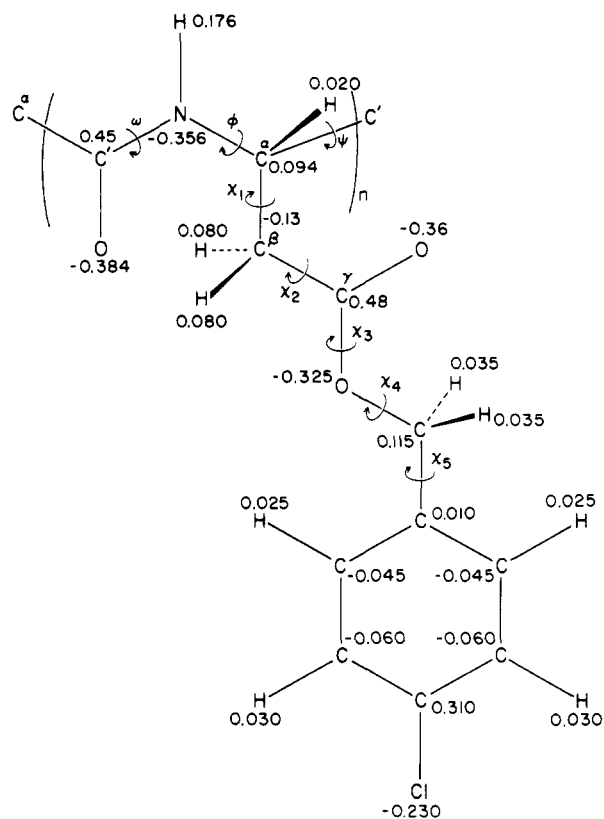


**Figure 2.** Dihedral angles and partial charges of the  $\beta$ -(*p*-chlorobenzyl)-L-aspartate residue in an *nmer*. The algebraic sum of the charges on the backbone and side chain of a residue is zero.

$$U_{el}(r_{ij}) = 332.0q_iq_j / Dr_{ij} \quad (3)$$

where  $q_i$  and  $q_j$  are the partial charges in electronic units obtained from semiempirical quantum mechanical CNDO/2 calculations<sup>5</sup> (see Figure 2), used with an apparent dielectric constant of  $D = 2$  according to McGuire *et al.*,<sup>5</sup>  $r_{ij}$  is the distance between the *i*th and *j*th atoms, and 332.0 is a factor to adjust the energy units to kcal/mol when  $r_{ij}$  is in Ångstrom units.

**C. Torsional Potentials.** Even though the torsional energies are poorly understood theoretically, they have been included in empirical energy calculations to account for interactions required to fit the observed energy barrier to rotation about single bonds. Thus, the torsional potential used in any calculation must be consistent with all other explicitly included interactions. Since we have introduced both new nonbonded parameters and partial charges, it became necessary to reevaluate our torsional potentials. For this purpose, we have utilized the results of Yan *et al.*<sup>26</sup> who have examined the barriers to internal rotation about single bonds by semiempirical quantum mechanical calculations. Assuming that these calculated barriers are the correct ones, we have evaluated the torsional potential function [with the dihedral angles of the model molecules<sup>26</sup> used here redefined to agree with the equivalent dihedral angle of the aspartate ester side chain (see Figure 2)] as follows. The dihedral angle under consideration was varied from  $-180$  to  $180^\circ$ , and the empirical energy was calculated by means of eq 1 and 3. The torsional potential energy is then defined as the difference between the quantum mechanical energy and the empirical energy by the equation

$$U_{tor}(\chi_i) = U_{MO}(\chi_i) - U_{nb}(\chi_i) - U_{el}(\chi_i) + C \quad (4)$$

where *i* defines the particular dihedral angle,  $U_{MO}$  the energy determined from the semiempirical quantum me-

chanical calculations,  $U_{nb}$  and  $U_{el}$  the summation of non-bonded and electrostatic interaction energies from eq 1 and 3, respectively, and  $C$  a constant used to normalize the minimum torsional potential energy to be zero. A torsional potential function to include all angles from  $-180$  to  $180^\circ$  was next generated by fitting these results to the following Fourier expansion

$$U_{\text{tor}}(\chi_i) = B_0 + \sum_{n=1} B_n \cos n\chi_i \quad (5)$$

The coefficients  $B_n$ ,  $n = 0, 1, 2 \dots$ , were determined by the method of least squares for different values of  $n$ , and the lowest value of  $n$  giving a good fit of the data was determined. The resulting functions (with all energies in kcal/mol) for the dihedral angles shown in Figure 2 are

$$U_{\text{tor}}(\chi_3) = 15.21 - 5.53 \cos \chi_3 - 6.42 \cos 2\chi_3 - 1.59 \cos 3\chi_3 \quad (6)$$

$$U_{\text{tor}}(\chi_4) = -0.62 - 4.39 \cos \chi_4 - 2.41 \cos 2\chi_4 - 2.28 \cos 3\chi_4 \quad (7)$$

and

$$U_{\text{tor}}(\chi_5) = 0.7(1 - \cos 2\chi_5) \quad (8)$$

For  $\chi_1$ , we use

$$U_{\text{tor}}(\chi_1) = 1 + \cos 3\chi_1 \quad (9)$$

and for  $\omega$  we use the value of McGuire *et al.*,<sup>3</sup> viz.

$$U_{\text{tor}}(\omega) = 10(1 - \cos 2\omega) \quad (10)$$

According to Momany *et al.*,<sup>5</sup> no torsional potentials are required for the variation of  $\phi$ ,  $\psi$ , and  $\chi_2$ .

**D. Energy Minimization.** The total (intra- and intermolecular) potential energy was minimized with respect to the dihedral angles,  $\Delta z$  and  $z_{\text{rot}}$  and the lattice constants, as before,<sup>3</sup> using the procedure of Scott *et al.*<sup>33</sup> Prior to minimization, all variables were divided into subsets, with each subset treated independently. For each minimization, only those energy terms which depend on the variables within a particular subset were summed. A final energy minimum is determined by a system of line searches and quadratic interpolations: The energies of the regular poly(amino acid) helices and of the crystal structures could be minimized with respect to all or any of the variables, as described elsewhere.<sup>3</sup>

**E. Entropy of Rotation.** Although one of the basic assumptions in the use of empirical energy functions to calculate the conformation of a macromolecule is that the observed conformation is the most stable one, *i.e.*, the one of highest statistical weight,<sup>34,35</sup> in practice the minimized potential energy has been used in most cases to predict the most stable conformation. Although this practice appears justified when applied to isolated regular homopolymers, as is indicated by the ability to correctly predict the helix sense for a large number of macromolecules,<sup>3,24-26,36</sup> the large amount of experimental evidence<sup>6,37-41</sup> showing freedom of motion about the helix axis in crystals suggests that this practice is not applicable to crystals of homopolymers. Therefore, we have included an entropy contribution in addition to the potential energy. Simply for the purpose of illustrating how the entropy influences the crystal packing, we include only the entropy for rotation of a homopolymer about its helix axis within a crystal lattice, and omit all other entropy contributions to the resulting Helmholtz conformational free energy.

For any set of lattice constants<sup>42</sup>  $a$ ,  $b$  and  $c$ , the Helm-

holtz conformational free energy<sup>35</sup> of the crystal is

$$F(a, b) = -RT \ln Z(a, b) \quad (11)$$

where  $T$  is the absolute temperature and  $R$  is the universal gas constant.  $Z(a, b)$  is the classical statistical mechanical conformational partition function of the crystal, and can be written as

$$Z(a, b) = \int \exp[-E(a, b, q_1, \dots, q_m)/RT] \prod_{i=1}^m dq_i \quad (12)$$

where  $m$  is the total number of degrees of freedom of the crystal (including both intra- and intermolecular degrees of freedom, but excluding  $a$ ,  $b$ , and  $c$ ),  $E(a, b, q_1, \dots, q_m)$  is the potential energy of the crystal as a function of  $a$ ,  $b$  and the generalized coordinates  $(q_1, \dots, q_m)$ , and the integration is carried out over the whole coordinate space. If we consider the crystal to be an assembly of regular homopolymers of infinite chain length, packed with perfect symmetry, and that each residue of a homopolymer in the crystal has the same environment, then the conformational partition function of a crystal containing a total of  $N$  residues can be simplified to

$$Z(a, b) = [Z_r(a, b)]^N \quad (13)$$

giving the following expression for the Helmholtz conformational free energy per residue

$$F_r(a, b) = -RT \ln Z_r(a, b) \quad (14)$$

where  $Z_r(a, b)$  is the conformational partition function of a residue, *viz.*

$$Z_r(a, b) = \int \exp[-E_r(a, b, q_1, \dots, q_p)/RT] \prod_{i=1}^p dq_p \quad (15)$$

with  $p = m/N$  being the number of degrees of freedom of each residue in the crystal, and  $E_r(a, b, q_1, \dots, q_p)$  is the potential energy per residue in the crystal as a function of  $a$ ,  $b$  and the generalized coordinates  $(q_1, \dots, q_p)$  associated with each residue. Since we take bond lengths and bond angles as fixed, the generalized coordinates  $(q_1, \dots, q_p)$  refer to the dihedral angles within the residue and the lattice coordinates, *i.e.*, the relative distances and orientations of the residues in the crystal. The integration in eq 15 is carried out over the whole coordinate space. However, the  $q$  space can be divided further into subspaces, each of which pertains to a particular type of conformation  $\rho$ . Integrating in eq 15 over each subspace, the partition function<sup>35</sup> becomes

$$Z_r(a, b) = \sum_{\rho} Z_{r\rho}(a, b) \quad (16)$$

where  $Z_{r\rho}$  is the partition function for a particular conformation. Since the X-ray diffraction study<sup>6</sup> indicates that  $p$ -Cl-PBLA exists in only two forms in fibers, *viz.*, the right-handed  $\alpha$  and  $\omega$  helices at low and high temperatures, respectively, we confine our considerations to only these two helical forms in their respective crystal symmetries. Thus, part of the Helmholtz conformational free energy per residue [for subspace  $\rho$  and lattice constant  $a$  (constrained to be equal to  $b$ , in accordance with the experimental data<sup>6</sup>)] is

$$F_{r\rho}(a, b) = -RT \ln Z_{r\rho}(a, b) \quad (17)$$

We may compare the relative stabilities of various structures  $\rho$  (taken here as  $\alpha$  and  $\omega$ , respectively) in their corresponding crystals, at a given temperature, by comparing the relative values of  $F_{r\rho}(a, b)$  which include various entropy contributions.

**Table I**  
**Conformations and Energies of Single  $\alpha$ -Helical Chains of *p*-Cl-PBLA**

Conformation <sup>a</sup>		Dihedral Angles (deg)							kcal/mol of Residue		
		$\phi$	$\psi$	$\chi_1$	$\chi_2$	$\chi_3$	$\chi_4$	$\chi_5$	$E_R^c$	$E_H^c$	$E_{total}$
Rt(–)	Initial <sup>b</sup>	–48.3	–57.0	–62.0	–56.5	–177.2	–85.5	171.6			
	Minimized <sup>c</sup>	–64.4	–42.5	–64.1	–69.9	160.3	–47.1	127.2	4.08	23.34	27.42
Rt(–)	Initial <sup>b</sup>	–50.6	–55.7	–57.5	–19.5	167.6	–142.6	161.8			
	Minimized <sup>c</sup>	–64.5	–41.4	–59.1	–36.3	143.0	–134.5	154.0	7.84	24.06	31.90
Lt(–)	Initial <sup>b</sup>	+46.1	+60.9	166.0	27.3	–156.1	152.8	14.2			
	Minimized <sup>c</sup>	+52.5	+60.2	–169.8	0.1	–140.3	154.5	33.9	9.67	22.19	31.86
Lt(+)	Initial <sup>b</sup>	+49.9	+57.0	–59.7	148.6	–161.6	84.9	3.3			
	Minimized <sup>c</sup>	+53.0	+57.8	–55.1	140.8	–158.2	48.8	57.3	4.35	23.82	28.17
T(R)	Initial <sup>d</sup>	–46.2	–57.6	–85.2	160.2	–157.1	158.1	–105.1			
	Minimized <sup>c</sup>	–63.2	–42.1	–63.3	150.8	–170.9	165.0	–34.9	9.53	24.50	34.03

<sup>a</sup> R and L denote right- and left-handed  $\alpha$  helices, respectively; t(+) and t(–) mean that the side chains are in a transverse conformation in which they wrap around the backbone in a clockwise (+) or counterclockwise (–) direction, when the helix is viewed from the N-terminal end. T is the conformation of Takeda *et al.*<sup>6</sup> <sup>b</sup> Starting conformations from Yan *et al.*<sup>26</sup> <sup>c</sup> Conformations and energies after minimization with respect to  $\phi$ ,  $\psi$ ,  $\chi$ 's, with  $\omega$  held fixed at 180°. <sup>d</sup> Starting conformation from Takeda *et al.*<sup>6</sup> <sup>e</sup>  $E_R$  and  $E_H$  are the intraresidue and helix energies, respectively.

Instead of calculating  $F_{rp}(a, b)$  by including the complete domain of the subspace  $\rho$  (which would be a very time-consuming computation), we limit ourselves to only one degree of freedom (as far as the entropy calculation is concerned) and keep the rest of the generalized coordinates at their values which correspond to a minimum in the potential energy. Our purpose in using this simplified model is solely to examine how the variation in a particular coordinate (*i.e.*, a particular entropy contribution) contributes to the stability of the crystal lattice. For simplicity, and because such motion is thought<sup>6,37–41</sup> to exist, we have chosen  $z_{rot}$  as the coordinate to vary. Furthermore, the homopolymers within the crystal lattice are assumed to rotate together in the same direction about the helix axis, so that the partition function per residue of structure  $\rho$ , allowing only for rotation of the helix about its axis, is

$$[Z_{rp}(a, b)]_{rot} = \int \exp[-E_{rp}(a, b, \{q_i^0\}_{i \neq z_{rot}}, z_{rot}) / RT] dz_{rot} \quad (18)$$

where  $\{q_i^0\}_{i \neq z_{rot}}$  is a set of all generalized coordinates of a residue (except  $z_{rot}$ ) at the minimum of the potential energy of the crystal for structure  $\rho$  and lattice constants  $a$  and  $b$ . In other words, the dihedral angles of each chain, the relative positions of the chains (except for  $z_{rot}$ ), and the lattice constants are kept at their equilibrium values, and  $z_{rot}$  is varied. The potential energy for any value of  $z_{rot}$  may be defined as

$$E_{rp}(a, b, \{q_i^0\}_{i \neq z_{rot}}, z_{rot}) = E_{rp}(a, b, \{q_i^0\}) + \Delta E(z_{rot}) \quad (19)$$

where  $E_{rp}(a, b, \{q_i^0\})$  is the minimum value of the potential energy for the homopolymers in a fixed lattice and  $\Delta E(z_{rot})$  is the change in energy due to a displacement of these fixed homopolymers from their position of minimum potential energy by rotations about their helix axis. Substituting eq 18 and 19 into eq 17, the Helmholtz conformational free energy per residue of structure  $\rho$  due to variation of  $z_{rot}$  at lattice constants  $a$  and  $b$  becomes

$$[F_{rp}(a, b)]_{rot} = E_{rp}(a, b, \{q_i^0\}) - RT \ln \left\{ \int \exp[-\Delta E(z_{rot}) / RT] dz_{rot} \right\} \quad (20)$$

In practice  $[F_{rp}(a, b)]_{rot}$  was calculated as follows. For each set of lattice constants ( $a$  and  $b$ ) (with the backbone conformation held fixed at the experimental one), the most stable crystal structure is obtained by a minimization of the total potential energy with respect to all side-chain dihedral angles,  $\Delta z$  and  $z_{rot}$ . This homopolymer

conformation is then held fixed and only  $z_{rot}$  is allowed to vary. A continuous expression for the energy difference is determined, and  $[F_{rp}(a, b)]_{rot}$  is obtained by eq 20. By repeating this calculation for several sets of values of  $a$  and  $b$ , the minimum in  $[F_{rp}(a, b)]_{rot}$  and hence the statistically most stable crystal structure (including this rotational freedom) is determined.

## Results and Discussion

**A. Isolated Helices.** Before packing the helices in crystals, we obtain the minimum-energy conformations of the isolated  $\alpha$  and  $\omega$  helices<sup>43</sup> of *p*-Cl-PBLA, using 18 and 4<sup>44</sup> residues for the  $\alpha$  and  $\omega$  helices, respectively; the resulting side-chain conformations are subsequently used in calculations on crystalline arrays of helices. The  $\omega$  helix differs from the  $\alpha$  helix in that it has 4.0 instead of 3.6 residues per turn.

For the  $\alpha$  helix, five side-chain starting conformations were taken; four were those of Yan *et al.*, which had been determined<sup>26</sup> with a different set of empirical energy functions, and the fifth was that of Takeda *et al.*<sup>6</sup> These are listed in Table I together with the conformations and energies computed by energy minimization with respect to  $\phi$ ,  $\psi$ , and the  $\chi$ 's (with  $\omega$  held fixed at 180°). The large positive values for the minimized energies arise primarily from the inclusion of 1–4 electrostatic interactions which had been omitted previously<sup>26</sup> and from the exclusion of 1–3 interactions which are attractive and do not vary with conformation. In agreement with Yan *et al.*,<sup>26</sup> we find the lowest-energy structure to be the one with the Rt(–) conformation, even with the new set<sup>4,5</sup> of energy functions, being 0.75 kcal/mol of residue more stable than the Lt(+) conformation. The differences in the ordering of the energies of the other conformations, compared to that of Yan *et al.*<sup>26</sup> is due to differences in the energy functions. Conformation T(R) of Takeda *et al.*<sup>6</sup> has too high an energy [by 6.6 kcal/mol of residue compared to that of Rt(–)] to exist as an isolated  $\alpha$  helix; this high energy arises mostly from an unfavorable side-chain orientation.

This new set of energy functions<sup>4,5</sup> was also used to compute the handedness of isolated  $\alpha$ -helical poly( $\beta$ -benzyl-L-aspartate). Using the four low-energy starting conformations of Yan *et al.*,<sup>25</sup> two right- and two left-handed helices, energy minimization showed that the left-handed helix is the most stable one, in agreement with experiment.<sup>7,8</sup>

In order to obtain appropriate starting side-chain conformations of the homopolymers for crystal packing, ener-

**Table II**  
**Conformations and Energies of Single  $\alpha$ - and  $\omega$ -Helical Chains of  $p$ -Cl-PBLA<sup>a</sup>**

Helix	Conformation <sup>b</sup>	Dihedral Angles (deg)								kcal/mol of Residue		
		$\omega$	$\phi^c$	$\psi^c$	$\chi_1$	$\chi_2$	$\chi_3$	$\chi_4$	$\chi_5$	$E_R^d$	$E_H^d$	$E_{total}$
$\alpha$	Rt(-)	180	-45.3	-58.1	-65.1	-84.5	147.8	-41.0	115.5	2.76	25.77	28.53
$\alpha$	T(R)	180	-45.3	-58.1	-67.6	152.4	-162.9	159.1	-34.9	8.81	28.21	37.02
$\omega$	Rt(-)	180	-34.2	-82.9	-82.2	-92.5	151.2	-42.5	119.2	4.01	38.72	42.73
$\omega$	Rt( $\omega$ )	-175.5	-62.2	-55.5	-63.1	-91.6	147.1	-40.1	116.1	2.96	26.08	29.04

<sup>a</sup> Computed with the constraint that  $h$  and  $t$  are fixed at 1.5 Å and 100° for the  $\alpha$  helix and at 1.3 Å and 90° for the  $\omega$  helix. 18 and 4 residues were used for the  $\alpha$  and  $\omega$  helices, respectively. <sup>b</sup> Starting side-chain conformations of Rt(-) and T(R) were from Table I; Rt(-) conformation refers to the first Rt(-) structure of Table I. <sup>c</sup> ( $\phi, \psi$ ) were calculated from ( $\omega, h, t$ ) using the Sugeta-Miyazawa equation.<sup>32</sup> <sup>d</sup>  $E_R$  and  $E_H$  are the intraresidue and helix energies, respectively.

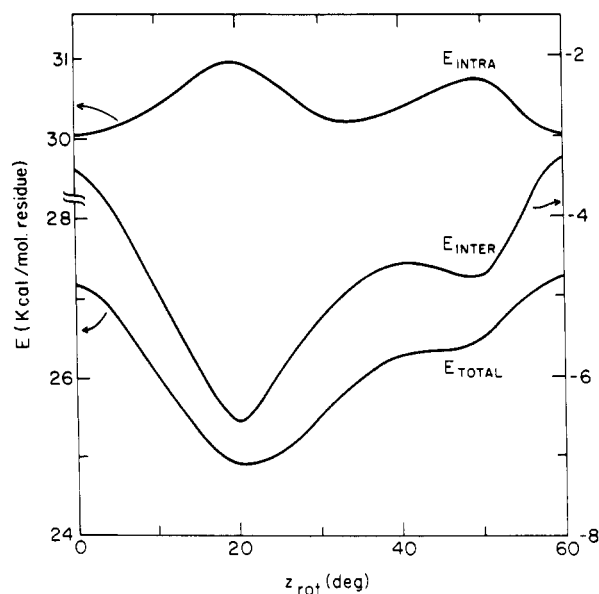


**Figure 3.** Values of  $E_{intra}$  and  $E_{inter}$  found when  $E_{total}$  is minimized with respect to the  $\chi_i$ 's at each value of  $z_{rot}$  for structure Rt(-) of  $\alpha$ -helical  $p$ -Cl-PBLA. The quantities  $a$ ,  $b$ ,  $c$ ,  $h$ , and  $t$  were held fixed at the experimental values, and  $\omega$  at 180°.

gy minimization was carried out on the isolated  $\alpha$  and  $\omega$  helices [but now including the constraint that the backbone reproduce the observed<sup>6</sup> values of  $h$  and  $t$  (1.5 Å and 100° for the  $\alpha$  helix, and 1.3 Å and 90° for the  $\omega$  helix)]. With  $\omega$  fixed at 180°, the values of  $\phi$  and  $\psi$  follow directly from those of  $h$  and  $t$  by means of the Sugeta-Miyazawa equations.<sup>32</sup> For the side chains, two starting conformations were considered for the  $\alpha$  helix and one for the  $\omega$  helix.<sup>45</sup> For the  $\alpha$  helix, these were the lowest-energy Rt(-) structure of Table I and the minimum-energy T(R) structure of Table I. For the  $\omega$  helix, the starting side-chain conformation was taken as that of the stable right-handed  $\alpha$ -helical structure<sup>26</sup> [Rt(-) of Table I].<sup>45</sup> The energy was minimized only with respect to the  $\chi_i$ 's, keeping  $\omega$ ,  $h$ , and  $t$  fixed. The resulting conformations and energies are shown in the first three lines of Table II. As in Table I, the  $\alpha$ -helical Rt(-) structure is again the one of lowest energy; however, structure T(R) becomes even less stable than in Table I. Furthermore, the most stable  $\alpha$  helix has a planar peptide group [ $\omega = 180^\circ$  for both Rt(-) and T(R) at the experimental values<sup>6</sup> of  $a = b = 14.9$  Å] as shown in Table VI. This, plus a test we carried out to show that the isolated  $\alpha$  helix of structure Rt(-) is more stable at  $\omega = 180^\circ$  than at  $179^\circ$ , provides a justification for our use of a planar peptide group for the  $\alpha$  helix throughout this paper. However, the large destabilization energy<sup>46</sup> of the  $\omega$  helix (14.2 kcal/mol of residue) arises primarily by constraining  $\omega$  to 180°. Hence, the minimization of the

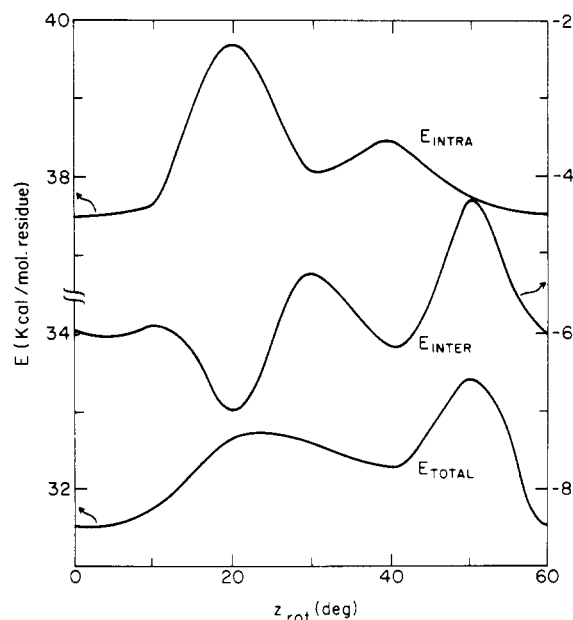


**Figure 4.** Same as Figure 3, but for structure T(R) of  $\alpha$ -helical  $p$ -Cl-PBLA.

energy of the  $\omega$  helix was repeated, starting from the conformation on the third line of Table II, but this time allowing  $\omega$  (as well as the  $\chi_i$ 's) to vary, keeping  $h$  and  $t$  fixed at the experimental values.<sup>6</sup> The results are shown in the fourth line of Table II. Despite the resulting non-planarity of the amide group ( $\omega = -175.5^\circ$ ), the energy is much lower; however, it is still higher than that of the Rt(-) helix by at least 0.51 kcal/mol of residue. The  $\omega$ -helix conformation in the fourth line of Table II [hereafter referred to as Rt( $\omega$ )] is the one which is packed in section C; since the energy increases sharply for positive and negative deviations of  $\omega$  from  $-175.5^\circ$ ,  $\omega$  would not be expected to be influenced by intermolecular forces in the crystal (as observed previously<sup>3</sup> for the  $\omega$  helix of  $p$ -PBLA), and therefore will be held fixed when the  $\omega$  helix is packed.

**B. Packed  $\alpha$ -Helical Structures of  $p$ -Cl-PBLA.** X-Ray diffraction studies of Takeda *et al.*<sup>6</sup> have shown that oriented fibers of  $p$ -Cl-PBLA prepared from a concentrated chloroform solution (at room temperature) form an  $\alpha$  helix with 18 residues in 5 complete turns. By analysis of 47 relatively sharp reflections, they were able to interpret their results by assuming a random distribution of up and down chains, and hence to determine that the conformation of the chain in the packed structure was a right-handed  $\alpha$  helix in a hexagonal lattice with  $\alpha = \beta = 90^\circ$ ,  $\gamma = 60^\circ$ ,  $a = b = 14.9$  Å, and  $c = 27.0$  Å. In addition, they were able to conclude that the Cl atom is located 6.5 Å from the helix axis.

Takeda *et al.*<sup>6</sup> also found that, if these fibers were heat-

**Table III**  
**Conformations and Energies of Packed  $\alpha$ -Helical Rt(-) Conformations<sup>a</sup> of *p*-Cl-PBLA**

$a = b$ (Å)	$z_{\text{rot}}^b$ (deg)	Dihedral Angles <sup>b</sup> (deg)					kcal/mol of Residue					
							$E_{\text{intra}}^c$		$E_{\text{inter}}^d$		$E_{\text{total}}$	$[F_{\text{r}\alpha}]_{\text{rot}}^e$
		$\chi_1$	$\chi_2$	$\chi_3$	$\chi_4$	$\chi_5$	$E_R$	$E_H$	$E_{\text{el}}$	$E_{\text{nb}}$		
12.0	23.8	-39.3	-103.4	165.9	-42.7	127.9	7.47	31.86	0.024	-10.08	29.28	28.64
13.0	23.4	-51.4	-89.9	153.2	-51.0	121.8	3.90	28.46	-0.16	-8.70	23.50	22.40
13.5	21.4	-58.5	-91.0	149.9	-49.5	119.8	3.16	28.13	-0.22	-8.15	22.92	22.14
14.0	20.0	-61.4	-92.8	149.4	-50.7	122.5	3.24	28.06	-0.24	-7.70	23.37	22.30
14.5	19.2	-68.4	-91.6	150.4	-51.0	124.3	3.52	27.78	-0.24	-7.26	23.80	22.54
14.9	17.3	-71.5	-94.6	151.0	-49.0	124.3	3.60	27.73	-0.25	-6.84	24.23	22.84
15.5	11.5	-71.2	-101.0	152.3	-49.7	125.6	3.67	27.91	-0.24	-5.97	25.37	23.40

<sup>a</sup> The backbone conformations were held fixed at  $h = 1.5$  Å,  $t = 100^\circ$ ,  $\phi = -45.3^\circ$ ,  $\psi = -58.1^\circ$ , and  $\omega = 180^\circ$ . <sup>b</sup> The side-chain dihedral angles and  $z_{\text{rot}}$  were varied during energy minimization from the initial conformation:  $\chi_1 = -66.4^\circ$ ,  $\chi_2 = -97.4^\circ$ ,  $\chi_3 = 151.6^\circ$ ,  $\chi_4 = -51.0^\circ$ ,  $\chi_5 = 124.3^\circ$ , and  $z_{\text{rot}} = 20^\circ$ , respectively. <sup>c</sup>  $E_{\text{intra}}$  is the sum of the intraresidue and helix energies,  $E_R$  and  $E_H$ , respectively. <sup>d</sup>  $E_{\text{el}}$  is the electrostatic energy, and  $E_{\text{nb}}$  is the nonbonded interaction energy. <sup>e</sup>  $[F_{\text{r}\alpha}]_{\text{rot}}$  is the Helmholtz conformational free energy per residue including the entropy contribution from the helix rotation, and is calculated at  $T = 300^\circ\text{K}$ .

**Table IV**  
**Conformations and Energies of Packed  $\alpha$ -Helical T(R) Conformations<sup>a</sup> of *p*-Cl-PBLA**

$a = b$ (Å)	$z_{\text{rot}}^b$ (deg)	Dihedral Angles <sup>b</sup> (deg)					kcal/mol of Residue				
							$E_{\text{intra}}^c$		$E_{\text{inter}}^d$		$E_{\text{total}}$
		$\chi_1$	$\chi_2$	$\chi_3$	$\chi_4$	$\chi_5$	$E_R$	$E_H$	$E_{\text{el}}$	$E_{\text{nb}}$	
12.0	13.6	-71.0	147.7	-140.2	151.1	-18.5	9.13	33.73	-0.24	-11.65	30.98
13.0	0.7	-68.4	146.7	-157.1	159.1	-16.7	8.98	29.49	-0.17	-8.78	29.52
13.5	0.0	-68.3	149.8	-156.6	159.1	-24.2	8.86	28.90	-0.14	-8.17	29.45
14.0	3.3	-72.2	152.4	-159.5	159.1	-28.1	9.01	28.57	-0.21	-7.61	29.76
14.5	2.9	-73.3	155.6	-160.3	158.5	-31.2	9.09	28.52	-0.18	-6.86	30.57
14.9	1.5	-70.7	157.6	-162.1	159.1	-34.7	8.99	28.48	-0.14	-6.06	31.27
15.5	2.9	-70.2	161.8	-156.1	159.1	-32.5	9.02	28.53	-0.21	-5.17	32.16

<sup>a</sup> The backbone conformations were held fixed at  $h = 1.5$  Å,  $t = 100^\circ$ ,  $\phi = -45.3^\circ$ ,  $\psi = -58.1^\circ$ , and  $\omega = 180^\circ$ . <sup>b</sup> The side-chain dihedral angles and  $z_{\text{rot}}$  were varied during energy minimization from the initial conformation:  $\chi_1 = -71.3^\circ$ ,  $\chi_2 = 157.6^\circ$ ,  $\chi_3 = -159.5^\circ$ ,  $\chi_4 = 159.1^\circ$ ,  $\chi_5 = -34.0^\circ$ , and  $z_{\text{rot}} = 0.0^\circ$ , respectively. <sup>c</sup>  $E_{\text{intra}}$  is the sum of the intraresidue and helix energies,  $E_R$  and  $E_H$ , respectively. <sup>d</sup>  $E_{\text{el}}$  is the electrostatic energy, and  $E_{\text{nb}}$  is the nonbonded interaction energy.

ed to  $190^\circ$ , the conformation of the chain was converted to an  $\omega$ -helical form. The  $\omega$  helices were found to be packed in a tetragonal unit cell with  $\alpha = \beta = \gamma = 90^\circ$ ,  $a = b = 23.3$  Å, and  $c = 5.20$  Å. We will consider the packing of  $\alpha$  helices in this section, and  $\omega$  helices in section C.

To calculate the crystal packing of the *p*-Cl-PBLA  $\alpha$  helix, the homopolymers were arranged within a hexagonal lattice by placing the reference helix (with 18 residues/unit cell) at the origin of the unit cell with its helix axis parallel to the  $c$  axis, and constructing other unit cells by simply translating this reference helix in the directions of the  $a$ ,  $b$ , and  $c$  axes;  $3 \times 3 \times 3$  unit cells were constructed. For crystals of this space group ( $P_{6_3}22$ ), there is only one chain per unit cell, and we have assumed that all helical chains run in the same direction.<sup>47</sup> Since the relative positions of equivalent atoms in corresponding molecules in a crystal with one molecule per unit cell are unaffected by a translational displacement along the  $c$  axis,  $\Delta z$  was held constant at 0.0 Å. Variation of the orientation of the homopolymers within each unit cell is accomplished by a rotation about the helix axis,  $z_{\text{rot}}$ .

To examine the effects of crystal packing on the orientation of the side chains in the homopolymer, the energies for structures Rt(-) and T(R) were first considered as a function of the helix rotation  $z_{\text{rot}}$ . For each value of  $z_{\text{rot}}$  considered here (between 0 and  $60^\circ$  because of the symmetry of packing in this space group), the energies were minimized with respect to the five side-chain  $\chi_i$ 's; holding the backbone conformation at that given in Table II and the lattice constants (*i.e.*,  $a$ ,  $b$ , and  $c$ ) fixed at their experimental values. The results for structures Rt(-) and

T(R) are shown in Figures 3 and 4, respectively, as the total potential energy  $E_{\text{total}}$ , the intermolecular crystal-packing energy,  $E_{\text{inter}}$ , and the intramolecular homopolymer energy,  $E_{\text{intra}}$  as a function of  $z_{\text{rot}}$ . It can be seen that, in both structures, favorable intermolecular interactions,  $E_{\text{inter}}$ , between the molecules (primarily side-chain-side-chain attractive interactions) tend to reorient the side chains so as to cause unfavorable intramolecular interactions, *i.e.*, the crystal packing tends to distort the homopolymer side-chain conformation from the minimum-energy conformation that it would assume in the isolated state. Moreover, by comparing the depths of the energy wells, these results show that the side-chain conformation for the Rt(-) model is more favorably disposed to intermolecular interactions within the crystal lattice than is structure T(R). For example, at  $z_{\text{rot}} = 20^\circ$  both structures are destabilized internally as indicated by  $E_{\text{intra}}$ , although in fact Rt(-) is destabilized less (0.9 kcal/mol of residue) than is structure T(R) (2.2 kcal/mol of residue), both energies being referred to zero at  $z_{\text{rot}} = 0^\circ$ . However, the largest energy change arises from  $E_{\text{inter}}$  for Rt(-) leading to a minimum in  $E_{\text{total}}$  at  $z_{\text{rot}} = 20^\circ$ ; for structure T(R), the change in  $E_{\text{inter}}$  is smaller than that in  $E_{\text{intra}}$ , and hence the value of  $E_{\text{total}}$  indicates that T(R) is not a low-energy structure at  $z_{\text{rot}} = 20^\circ$ . One can also conclude from the most favorable conformation, *i.e.*, the one with the lowest total energy both for Rt(-) ( $E_{\text{total}} = 24.90$  kcal/mol of residue at  $z_{\text{rot}} = 20^\circ$ ) and for T(R) ( $E_{\text{total}} = 31.50$  kcal/mol of residue at  $z_{\text{rot}} = 0^\circ$ ), that crystal packing of these molecules in this particular lattice results in a stabilization of both conformations over

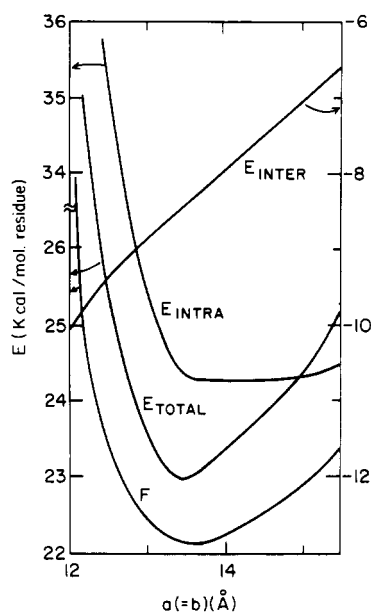


**Figure 5.** Values of  $E_{\text{intra}}$  and  $E_{\text{inter}}$  when  $E_{\text{total}}$  is minimized with respect to the  $\chi_i$ 's and  $z_{\text{rot}}$  at each value of  $a (= b)$  for structure Rt(-) of  $\alpha$ -helical *p*-Cl-PBLA. The quantities  $c$ ,  $h$ , and  $t$  were held fixed at the experimental values and  $\omega$  at  $180^\circ$ . The free energy  $F$  was computed by means of eq 20.

that in the free state by  $\sim 6.0$  kcal/mol of residue (in  $E_{\text{inter}}$ ). The values of the  $\chi_i$ 's in these minimum-energy Rt(-) and T(R) conformations are  $(-66.4^\circ, -97.4^\circ, 151.6^\circ, -51.0^\circ, 124.3^\circ)$  and  $(-71.3^\circ, 157.6^\circ, -159.5^\circ, 159.1^\circ, -34.0^\circ)$ , respectively.

To evaluate how the size of the crystal lattice affects the stabilization of both conformations over those in the free state, the total energies of packed structures of Rt(-) and T(R) were minimized with respect to the five  $\chi_i$ 's and  $z_{\text{rot}}$  at various values of  $a$  (constrained to be equal to  $b$ ) for fixed  $c$ ,  $h$ , and  $t$  (and  $\phi$ ,  $\psi$ ,  $\omega$ ). The starting conformations (shown in Tables III and IV) of the side chains in structures Rt(-) and T(R) were the values of the  $\chi_i$ 's at the minimum of  $z_{\text{rot}}$  in Figures 3 and 4, respectively, and the results are shown in Figures 5 and 6, respectively. In Figure 5, the minimum value of  $E_{\text{total}}$  for structure Rt(-) occurs at  $a = b = 13.5$  Å.  $E_{\text{intra}}$  increases sharply at smaller values of  $a$  and  $b$  because of strong nonbonded intramolecular repulsions as the side chains fold back on the backbone. For values of  $a$  and  $b$  greater than 13.5 Å,  $E_{\text{intra}}$  remains constant but  $E_{\text{inter}}$  (and hence  $E_{\text{total}}$ ) increases. Thus, the side chains adopt a most favorable conformation to maximize intermolecular attractions without introducing nonbonded intramolecular repulsions. As in Figure 3, where  $a$ ,  $b$ , and  $c$  were held constant, the stabilization arises from the intermolecular interactions. In fact, as shown in Table III, the intermolecular nonbonded attractions play the major role in stabilizing the Rt(-) structure in the crystal, even though the C—Cl dipole might have been expected to contribute electrostatic stabilization. In Figure 6, the minimum value of  $E_{\text{total}}$  for structure T(R) also occurs at  $a = b = 13.5$  Å, but this structure is 6.5 kcal/mol of residue less stable than structure Rt(-).  $E_{\text{intra}}$ ,  $E_{\text{inter}}$ , and  $E_{\text{total}}$  in Figure 6 behave qualitatively the same as in Figure 5, and therefore the same conclusions can be drawn. The interaction energies are given in Table IV, and again show the importance of the intermolecular nonbonded energy.

For each set of  $a$  and  $b$ , the Helmholtz conformational free energy per residue (including the rotational freedom) of packed structures of Rt(-) was computed by means of

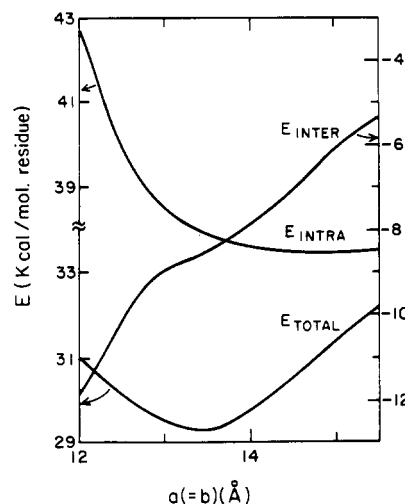


**Figure 6.** Same as Figure 5 (with omission of  $F$ ), but for structure T(R) of  $\alpha$ -helical *p*-Cl-PBLA.

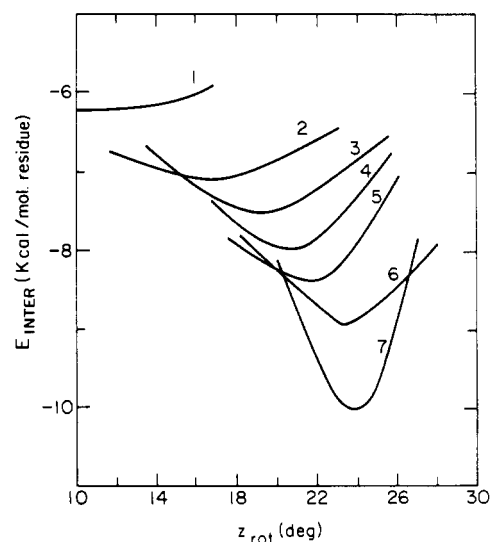


**Figure 7.** The dependence of  $E_{\text{inter}}$  on  $z_{\text{rot}}$  [around the minimum point ( $z_{\text{rot}}^0$ )] for structure Rt(-) of  $\alpha$ -helical *p*-Cl-PBLA for the following values of the lattice constants  $a (= b)$ : (1) 15.5, (2) 14.9, (3) 14.5, (4) 14.0, (5) 13.5, (6) 13.0, and (7) 12.0 Å. The parameters  $c$ ,  $h$ , and  $t$  were held fixed at the experimental values and  $\omega$  at  $180^\circ$ , and the  $\chi_i$ 's were fixed for a given value of  $a (= b)$ , corresponding to the minimum in  $z_{\text{rot}}$ .

eq 20, *viz.*, by allowing for variation of  $z_{\text{rot}}$  around the minimum-energy value found in this crystal lattice; *i.e.*, using the minimum-energy conformations at various values of  $a (= b)$ , listed in Table III for Rt(-),  $E_{\text{total}}^{48}$  was computed as a function of  $z_{\text{rot}}$  for fixed (minimum-energy)  $\chi_i$ 's  $c$ ,  $h$ , and  $t$  (and  $\phi$ ,  $\psi$ ,  $\omega$ ), and the results<sup>49</sup> are shown in Figure 7, where each curve corresponds to a different set of  $\chi_i$ 's and  $a (= b)$ . Curve 2 of Figure 7 differs from Figure 3 since the  $\chi_i$ 's of Figure 3 change in the subsequent minimization of Figure 7. At each value of  $z_{\text{rot}}$ , the energy deviation  $\Delta E(a, b, z_{\text{rot}})$  from the minimum value of  $E_{\text{total}}(a, b, z_{\text{rot}}^0)$  was determined from Figure 7 and eq 19, and the Helmholtz conformational free energy was computed using eq 20. The results are shown in Figure 5 and Table III. It can be seen that the curves become shallower as  $a (= b)$  increases; *i.e.*, for the larger lattice constants, there is more rotational freedom, and hence a larger entropy contribution to the free energy. This effect would increase the equilibrium size of the lattice. From Figure 5 and Table III, it can be seen that, whereas the

**Table V**  
**Directions of Transition Moment with Respect to Helix Axis for *p*-Cl-PBLA**

Structure	Helix	$a = b$ (Å)	Angle of Transition Moment with Respect to the Helix Axis (deg)			$r_{Cl}^d$ (Å)
			C=O <sup>a</sup>	C—O—C <sup>b</sup>	Phenyl <sup>c</sup>	
Experiment <sup>6</sup>	$\alpha$	14.9	59	46	71	6.5
Rt(-) <sup>e</sup>	$\alpha$	13.5	40	72	85	5.9
Rt(-) <sup>f</sup>	$\alpha$	13.93	39	73	90	6.2
Rt(-) <sup>e</sup>	$\alpha$	14.9	34	81	79	6.7
Rt(-) <sup>g</sup>	$\alpha$	14.9	37	80	82	6.5
T(R) <sup>e</sup>	$\alpha$	13.5	62	33	71	5.6
T(R) <sup>e</sup>	$\alpha$	14.9	67	37	61	6.4
Rt( $\omega$ ) <sup>e</sup>	$\omega$	21.6	34	84	79	6.7
Rt( $\omega$ ) <sup>e</sup>	$\omega$	23.3	49	77	78	7.3

<sup>a</sup> Transition moment lies at 19° to the C=O bond inclined toward the adjacent C <sup>$\beta$</sup> —C <sup>$\gamma$</sup>  bond. <sup>b</sup> Transition moment lies at 90° to the C=O bond in the plane of the COO group. <sup>c</sup> Transition moment is perpendicular to the phenyl ring. <sup>d</sup> The distance between the heavy Cl atom and the helix axis. <sup>e</sup> Structures Rt(-) of the second and fourth lines, and T(R) of  $\alpha$ -helical *p*-Cl-PBLA are those from Tables III and IV, respectively, while structure Rt( $\omega$ ) of the  $\omega$  helix is obtained from Table VII. The backbone conformations of these structures were held fixed at the experimental values. <sup>f</sup> Structure Rt(-) of the third line is the conformation corresponding to the equilibrium lattice constants  $\langle a \rangle = \langle b \rangle = 13.93$  Å. <sup>g</sup> Structure Rt(-) of the fifth line is from Table VI; the total energy was also minimized with respect to the backbone dihedral angles.

minimum in  $E_{total}$  occurs at  $a = 13.5$  Å, that in  $F$  occurs at  $a = 13.75$  Å. In order to obtain a more realistic assessment of the entropy associated with  $z_{rot}$  and  $a$  (constrained to be equal to  $b$ ), the weighted-average value of  $a$  was approximated as<sup>48</sup>

$$\langle a \rangle = \langle b \rangle = \frac{\int \int a \exp[-E_{total}/RT] da dz_{rot}}{\int \int \exp[-E_{total}/RT] da dz_{rot}} = \frac{\int a \exp\{-[F_{rot}(a,b)]_{rot}/RT\} da}{\int \exp\{-[F_{rot}(a,b)]_{rot}/RT\} da} \quad (21)$$

By using eq. 21, we obtain a further expansion of the equilibrium lattice to  $a = b = 13.93$  Å. Thus, the entropy contribution increases the computed equilibrium value of  $a$  ( $= b$ ) above that obtained in the minimization of  $E_{total}$ . Presumably the introduction of additional entropy contributions, arising from internal rotational freedom of the backbone and side-chain dihedral angles, bending of the helix, and a random up-and-down arrangement of the chains would increase the computed value of  $a$  further—in the direction of the observed value of 14.9 Å.

The computed distance between the heavy Cl atom and the helix axis increases monotonically with increasing  $a$  ( $= b$ ) for fixed  $c$ ,  $h$ , and  $t$  (and  $\phi$ ,  $\psi$ ,  $\omega$ ) as the  $\chi$ 's and  $z_{rot}$  vary, i.e., the side chains stretch out as the lattice expands to accommodate more extended side-chain conformations. At each  $a$  ( $= b$ ), the Cl atom is closer to the helix axis in structure T(R) compared to Rt(-). For Rt(-), this distance was found to be 6.7 Å at  $a = b = 14.9$  Å and decreases to 6.2 Å at  $a = b = 13.93$  Å. The experimental value<sup>6</sup> is 6.5 Å.

From infrared dichroism Takeda *et al.*<sup>6</sup> concluded that the transition moment of the CH out-of-plane vibration of the benzene ring (which is normal to the benzene ring) is inclined at 71° to the helix axis, and that the transition moments of the C=O stretching and C—O—C antisymmetric stretching vibrations are inclined at 59 and 46°, respectively, to the helix axis.<sup>50</sup> Using the geometry of the Rt(-) and T(R) structures in Tables III and IV, the orientations of the transition moments of various minimum-energy conformations were calculated and listed in Table V. At  $a = b = 13.5$  and 14.9 Å, both minimum-energy structures of Rt(-) and T(R) have values for the directions of the transition moment of the phenyl ring which are in good agreement with the experimental value.<sup>6</sup> The values for the ester group in T(R) agree better with experiment at  $a = b = 13.5$  and 14.9 Å than do those of Rt(-)

because T(R) was constructed<sup>6</sup> to fit these experimental values (taking the direction of the transition moment within the chromophore from model compounds). Considering that several factors can influence the direction of the transition moment, we regard the agreement between the calculated and observed transition moments of structure Rt(-) as good. These factors are: (a) the direction of the transition moment within the ester group of *p*-Cl-PBLA may differ from that in model compounds because of different environments;<sup>51-53</sup> (b) distortion of the transition moments by strong dipole-dipole interaction between the side-chain ester and backbone amide groups, and by the intermolecular interactions shown in Figures 8 and 9 for structure Rt(-); (c) influence of random up-and-down orientation of chains on both the calculated and observed values; and (d) restriction to fixed bond lengths and bond angles, and imposition of regularity condition, in the calculations.

In a final calculation on the  $\alpha$ -helical structures, the restriction to a fixed backbone conformation was removed to determine if a distortion of the  $\alpha$ -helix conformation would influence the crystal packing. The energies of the conformations corresponding to the values of  $E_{total}$  for three lattice conformations of Rt(-) ( $a = b = 13.5$ , 14.5, and 14.9 Å) and of two of T(R) ( $a = b = 13.5$  and 14.9 Å) from Tables III and IV, respectively, were minimized with respect to  $\phi$ ,  $\psi$ ,  $\omega$ ,  $\chi$ 's, and  $z_{rot}$  (holding the lattice constants  $a$  and  $b$  fixed). In this calculation, only  $3 \times 3 \times 1$  unit cells (with only one unit cell along the helix axis) were included, which makes the calculation less reliable.<sup>54</sup> This is a type of two-dimensional crystal where the third dimension along the helix axis is allowed to vary, without placing any restriction on  $c$ ,  $h$ , and  $t$  (or on  $\phi$ ,  $\psi$ , and  $\omega$ ). The results are shown in Table VI. Since the interactions between neighboring cells along the  $c$  axis are missing in this two-dimensional model, it is difficult to make a direct correct comparison between the energies in Table VI and those in Tables III and IV. However, some inferences can still be drawn from Table VI. First, the energy of Rt(-) is still lower than that of T(R), as was found for both the isolated helices and for the three-dimensional packed crystal structure. Second, the energy is lower for structures Rt(-) and T(R) at an expanded lattice, i.e., at the experimental lattice constants  $a = b = 14.9$  Å. This seems to support our earlier suggestion that the lattice constants would be increased if the backbone dihedral angles were allowed to vary. Third, as the lattice



**Table VI**  
**Conformations and Minimum Energies<sup>a</sup> of  $\alpha$ -Helical *p*-Cl-PBLA in Structures Rt(-) and T(R)**

Structure	$a = b^b$ ( $\text{\AA}$ )	Backbone Conformation					kcal/mol of Residue				
		$h$ ( $\text{\AA}$ )	$t^e$	$\phi^e$	$\psi^e$	$\omega^e$	$E_{\text{intra}}$		$E_{\text{inter}}$		$E_{\text{total}}$
							$E_R$	$E_H$	$E_{\text{el}}$	$E_{\text{nb}}$	
Rt(-)	13.5	1.8	112.0	-50.6	-36.8	180.0	3.26	28.42	0.12	-8.01	23.79
Rt(-)	14.5	1.4	100.5	-55.1	-49.4	178.0	3.58	24.80	-0.25	-7.67	20.46
Rt(-) <sup>c</sup>	14.9	1.4	98.7	-61.5	-45.7	180.0	3.97	24.06	-0.29	-7.50	20.24
T(R)	13.5	1.5	100.6	-45.7	-57.2	179.6	9.12	28.01	-0.17	-8.08	28.88
T(R) <sup>d</sup>	14.9	1.5	101.1	-58.9	-44.5	180.0	9.46	25.07	-0.22	-5.93	28.38

<sup>a</sup> For variable backbone conformation in two different size lattices.  $E_{\text{total}}$  was minimized with respect to the three backbone dihedral angles,  $\phi$ ,  $\psi$ , and  $\omega$ , five side-chain dihedral angles  $\chi_i$ 's, and the helix rotation angle  $z_{\text{rot}}$  ( $a$  and  $b$  were held fixed). <sup>b</sup> Initial side-chain conformations before minimization were those from Tables III and IV, while the initial backbone dihedral angles were  $\phi = -45.3^\circ$ ,  $\psi = -58.1^\circ$ , and  $\omega = 180.0^\circ$ , which are computed from the Sugeta-Miyazawa equations by using  $t = 100^\circ$  and  $h = 1.5 \text{ \AA}$ . <sup>c</sup> Minimum-energy side-chain dihedral angles are:  $\chi_1 = -70.6^\circ$ ,  $\chi_2 = -97.9^\circ$ ,  $\chi_3 = 151.6^\circ$ ,  $\chi_4 = -48.8^\circ$ , and  $\chi_5 = 121.3^\circ$ . <sup>d</sup> Minimum-energy side-chain dihedral angles are:  $\chi_1 = -69.8^\circ$ ,  $\chi_2 = 157.6^\circ$ ,  $\chi_3 = -161.5^\circ$ ,  $\chi_4 = 159.1^\circ$ , and  $\chi_5 = -31.2^\circ$ . <sup>e</sup> In degrees.

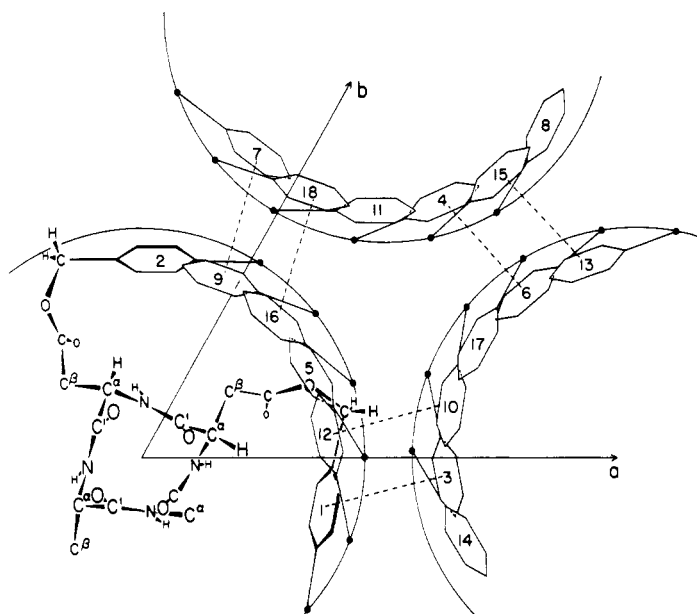


**Figure 8.**  $a - b$  projection of three packed Rt(-) chains of  $\alpha$ -helical *p*-Cl-PBLA in the minimum-energy conformation at  $a = b = 13.5 \text{ \AA}$  of Table III, showing the arrangement of the *p*-chlorobenzyl groups (numbered serially from the N to C terminus). For clarity, the backbone atoms of only four residues and the side-chain atoms of two residues in the reference chain are shown. The dashed lines indicate the nearest stacking of *p*-chlorobenzyl groups of adjacent chains. The chlorine atoms are indicated by solid circles.

constants are increased, the largest factor which lowers  $E_{\text{total}}$  is the lowering of  $E_H$ . Fourth, the changes in  $\phi$  and  $\psi$  or  $h$  and  $t$  imply that the new minimum-energy conformation occurs with only a small distortion from an ideal  $\alpha$  helix; at  $a = b = 14.9 \text{ \AA}$ , the unit cell length  $c$  (for 18 residues) along the helix axis becomes  $25.2 \text{ \AA}$ , which is shorter than the observed value<sup>6</sup> of  $27.0 \text{ \AA}$ . Moreover, 18 residues miss forming 5 complete turns by  $23.4^\circ$ . Fifth, the small changes in the directions of the transition moments and of the Cl atom distance shown in Table V imply that the side-chain conformation is conserved when the backbone conformation is varied.

In conclusion, structure Rt(-) (found by Yan *et al.*<sup>26</sup> to be the most stable isolated  $\alpha$ -helical one) fits best in the observed crystal, requiring only a slight modification of its side-chain conformation (see Tables III and V). This structure is more stable than the structure T(R) derived from the X-ray data. The stabilizing forces arising from

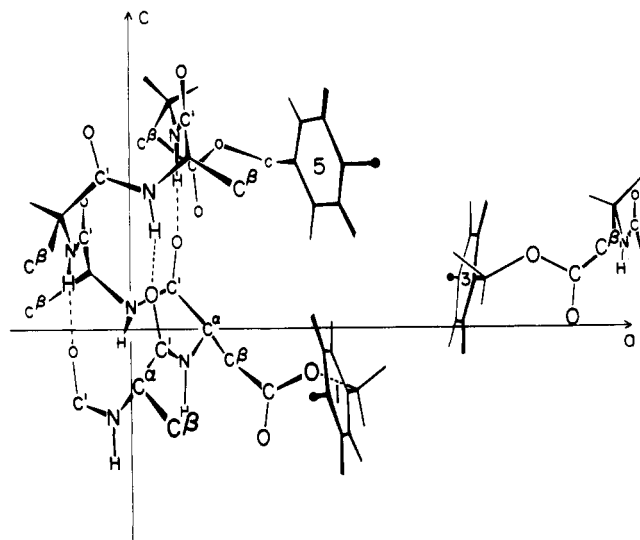


**Figure 9.**  $a - c$  projection of two packed Rt(-) chains of  $\alpha$ -helical *p*-Cl-PBLA in the minimum-energy conformation at  $a = b = 13.5 \text{ \AA}$  of Table III, showing the arrangement of the *p*-chlorobenzyl groups (numbered serially from the N to C terminus). For clarity, the backbone atoms of only five residues and the side-chain atoms of two residues (1 and 5) in the reference chain, and the *p*-chlorobenzyl groups of one other, are shown. The dashed lines indicate intramolecular hydrogen bonding. The chlorine atoms are indicated by solid circles.

crystal packing are primarily the nonbonded interactions, as also found in our previous studies of poly(L-alanine) and PBLA,<sup>3</sup> and not the electrostatic interactions as may have been anticipated. For the crystal packing of the  $\alpha$  helix, it is suggested (from the data of Table VI) that the side chains are reoriented to such an extent that the backbone conformation is slightly distorted to acquire additional stability. Models of these packed structures (Figures 8 and 9) show how the *p*-chlorophenyl groups of adjacent polymers appear to stack, with the first and 12th group of one molecule stacking with the third and tenth group of the closest neighbor at a distance of  $4.2 \text{ \AA}$ . Furthermore, the benzyl  $\text{CH}_2$  groups appear to interact with the *p*-chlorophenyl groups of adjacent chains, with no appreciable interaction of these *p*-chlorophenyl groups with one another within the same macromolecule. Finally, the intramolecular backbone hydrogen bonds were observed to occur at an  $\text{N} \cdots \text{O}$  distance of  $2.84 \text{ \AA}$ .

**C. Packed  $\omega$ -Helical Structures of *p*-Cl-PBLA.** As stated earlier, when  $\alpha$ -helical *p*-Cl-PBLA fibers are heated to  $190^\circ$ , they assume an  $\omega$ -helical conformation with a

**Table VII**  
**Conformations and Minimum Energies of Packed  $\omega$ -Helical Rt( $\omega$ ) Conformations<sup>a</sup> of *p*-Cl-PBLA**

$a = b$ (Å)	$z_{\text{rot}}^b$ (deg)	$\Delta z$ (Å)	Dihedral Angles (deg)					kcal/mol of Residue					
			$\chi_1$	$\chi_2$	$\chi_3$	$\chi_4$	$\chi_5$	$E_{\text{intra}}^c$		$E_{\text{inter}}^d$		$E_{\text{total}}$	$[F_{\text{rot}}]_{\text{rot}}^e$
								$E_R$	$E_H$	$E_{\text{el}}$	$E_{\text{nb}}$		
21.3	80.0	0.24	-79.5	-84.8	148.1	-49.5	107.0	5.08	27.15	0.49	-6.99	25.73	23.91
21.6	78.2	0.38	-73.6	-92.6	151.4	-43.5	118.4	3.94	27.15	0.51	-6.98	24.61	22.78
21.8	78.3	-0.21	-76.4	-90.0	153.9	-42.2	118.3	4.39	27.19	0.57	-7.39	24.76	22.85
22.3	75.4	-0.03	-76.4	-91.6	156.5	-43.5	123.2	4.57	27.26	0.51	-7.06	25.28	23.38
23.3	73.1	-0.32	-71.6	-112.0	153.9	-40.5	122.2	4.31	27.44	0.35	-5.89	26.20	24.18
24.3	75.0	-0.20	-71.4	-111.8	157.9	-46.0	129.1	4.56	27.51	0.24	-4.53	27.78	25.63

<sup>a</sup> The backbone conformations were held fixed at  $h = 1.3$  Å,  $t = 90^\circ$ ,  $\phi = -61.1^\circ$ ,  $\psi = -46.7^\circ$ , and  $\omega = -175.5^\circ$ .

<sup>b</sup> The energies are minimized from the initial conformations:  $\chi_1 = -83.5^\circ$ ,  $\chi_2 = -91.6^\circ$ ,  $\chi_3 = 153.9^\circ$ ,  $\chi_4 = -42.2^\circ$ ,  $\chi_5 = 120.4^\circ$ ,  $z_{\text{rot}} = 75^\circ$  and  $\Delta z = 0.016$  Å, taken from the minimum-energy conformation of Figure 10. <sup>c</sup>  $E_{\text{intra}}$  is the sum of the intraresidue and helix energies,  $E_R$  and  $E_H$ , respectively. <sup>d</sup>  $E_{\text{el}}$  is the electrostatic energy, and  $E_{\text{nb}}$  is the nonbonded energy. <sup>e</sup>  $[F_{\text{rot}}]_{\text{rot}}$  is the Helmholtz conformational free energy per residue including the entropy contribution from helix rotation, and is calculated at  $T = 463^\circ\text{K}$ .

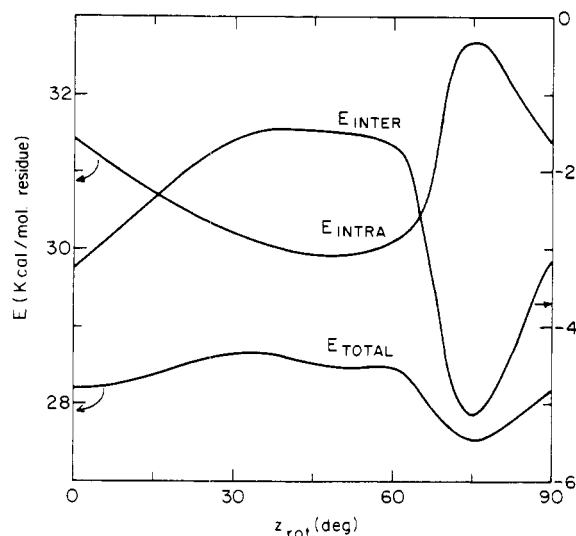


**Figure 10.** Values of  $E_{\text{intra}}$  and  $E_{\text{inter}}$  when  $E_{\text{total}}$  is minimized with respect to the  $\chi_i$ 's and  $\Delta z$  at each value of  $z_{\text{rot}}$  for structure Rt( $\omega$ ) of  $\omega$ -helical *p*-Cl-PBLA. The quantities  $a$ ,  $b$ ,  $c$  were held fixed at the experimental values, and the backbone conformation is that given in line 4 of Table II.

rearrangement of the unit cell, becoming tetragonal with the dimensions  $\alpha = \beta = \gamma = 90^\circ$ ,  $a = b = 23.3$  Å, and  $c = 5.20$  Å. We investigate here the packing energy in this crystal, compared to that of the low-temperature form in order to account for this observed conformational thermal transition in the fiber.

To calculate the crystal packing of the *p*-Cl-PBLA  $\omega$  helix, the homopolymers with four residues per chain [i.e., conformation Rt( $\omega$ ), in the last line of Table II] were arranged within a tetragonal lattice in the space group  $P_{4_2}2_1$  having two antiparallel chains in the unit cell. The reference helix was placed at the origin of the unit cell with its helix axis parallel to the  $c$  axis, and the second chain was generated by inverting the reference chain and translating it by  $a/2$ ,  $b/2$ , and  $c$  so that the chain points in the  $-c$  direction. Other unit cells were constructed by translating the reference unit cell in the  $a$ ,  $b$ , and  $c$  directions, to include  $3 \times 3 \times 3$  cells (or a chain length of 12 residues.<sup>44</sup> along the  $c$  axis) in the calculations, preserving the lattice symmetry. The relative orientations of the polymer chains within the unit cell can be adjusted by rotation about the helix axis by a rotation  $z_{\text{rot}}$ , and by translation of one helix in the unit cell with respect to the other by  $\Delta z$  along the  $c$  axis. As a result, any two closest neighboring helix chains rotate in opposite direction when  $z_{\text{rot}}$  is varied.

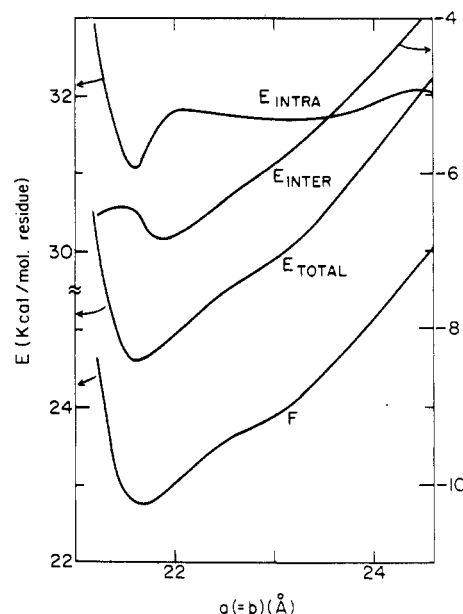


**Figure 11.** Values of  $E_{\text{intra}}$  and  $E_{\text{inter}}$  when  $E_{\text{total}}$  is minimized with respect to the  $\chi_i$ 's,  $\Delta z$ , and  $z_{\text{rot}}$  at each value of  $a (= b)$  for structure Rt( $\omega$ ) of  $\omega$ -helical *p*-Cl-PBLA. The quantities  $c$ ,  $h$ , and  $t$  were held fixed at the experimental values and  $\omega$  at  $-175.5^\circ$ . The free energy  $F$  was computed by means of eq 20.

To examine the effects of crystal packing on the orientation of the side chains in the homopolymer, the energies of packed Rt( $\omega$ ) helices were minimized with respect to the five  $\chi_i$ 's and  $\Delta z$ , for each value of  $z_{\text{rot}}$  between 0 and  $90^\circ$  (because of the tetragonal symmetry), holding the backbone conformation at that given in Table II, line 4, and the lattice constants (i.e.,  $a$ ,  $b$ , and  $c$ ) fixed at their experimental values.<sup>55</sup> The results are shown in Figure 10. The minimum in  $E_{\text{total}}$  occurs at  $z_{\text{rot}} = 75^\circ$  and  $\chi_i$ 's =  $(-83.5, -91.6, 153.9, -42.2, 120.4^\circ)$  and  $\Delta z = -0.016$  Å. As in the case of packed  $\alpha$  helices, the minimum in  $E_{\text{total}}$  corresponds to that in  $E_{\text{inter}}$ , even though  $E_{\text{intra}}$  is a maximum at this value of  $z_{\text{rot}}$ . This indicates that the side-chain conformations in the crystal change primarily in response to intermolecular interactions, despite unfavorable intrahelical interactions. Again, the dominant intermolecular energies are the nonbonded ( $-5.52$  kcal/mol of residue) and not the electrostatic interactions ( $0.38$  kcal/mol of residue).

To evaluate how the size of the crystal lattice affects the stabilization of the  $\omega$  helix over that in the free state, the total energy of the packed structure of Rt( $\omega$ ) was min-

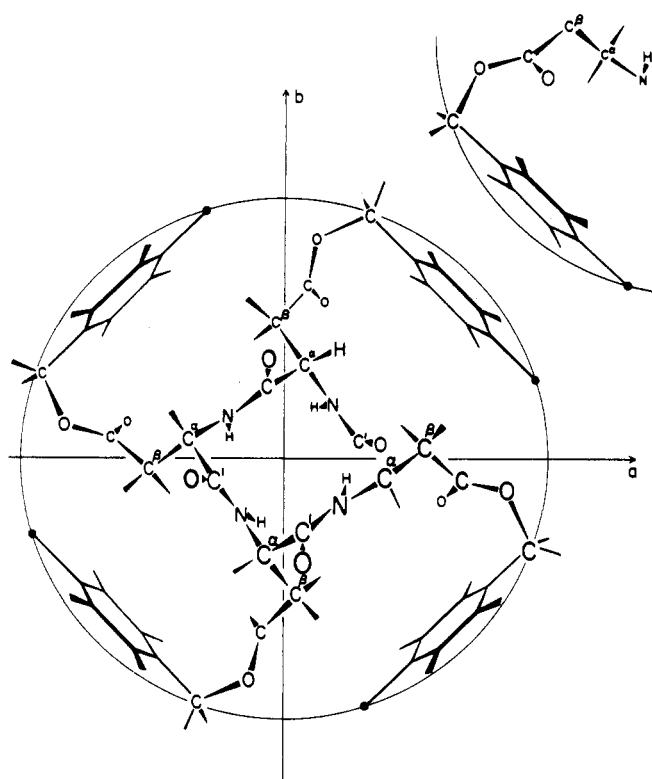


**Figure 12.** An  $a-b$  projection of two packed antiparallel  $Rt(\omega)$  chains of  $\omega$ -helical  $p$ -Cl-PBLA in the minimum-energy conformation at  $a = b = 21.6$  Å of Table VII, showing the arrangement of the  $p$ -chlorobenzyl groups. For clarity, the atoms of four residues of one complete helix turn in the reference chain and the atoms of one residue of the other chain in the same unit cell are shown. The chlorine atoms are indicated by solid circles.

imized with respect to the five  $\chi_i$ 's,  $\Delta z$ , and  $z_{rot}$  at various values of  $a$  (constrained to be equal to  $b$ ) for fixed  $c$ ,  $h$ , and  $t$  (and  $\phi$ ,  $\psi$ ,  $\omega$ ), starting with  $\chi_i$ 's =  $(-83.5, -91.6, 153.9, -42.2, 120.4^\circ)$ ,  $\Delta z = -0.016$  Å and  $z_{rot} = 75^\circ$ . The results are shown in Figure 11, with the conformations and energies listed in Table VII. The computed minimum in  $E_{total}$  occurs at  $a = b = 21.6$  Å. Above  $a = b = 22$  Å,  $E_{inter}$  becomes unfavorable; below  $a = b = 21.6$  Å, the interatomic overlap within the same molecule (included in  $E_{intra}$ ) prevents a closer approach of the helices. Between 21.5 and 22 Å, the data of Table VII indicate that  $\Delta z$  changes abruptly and the  $\chi_i$ 's change so that the side-chain benzyl groups of one molecule stack with those of its neighbor. In this way,  $E_{nb}$  from intermolecular contacts (and not  $E_{el}$  which is repulsive) plays a dominant role in achieving the new packing arrangement (which is more tightly packed for the  $\omega$  helix compared to the  $\alpha$  helix in agreement with the experimental observations<sup>6</sup>).

The rotational entropy of the  $\omega$ -helix (arising from a variation in  $z_{rot}$  around the minimum-energy conformation of Table VII) at each  $a$  ( $= b$ ) was computed in the same manner as for the  $\alpha$  helix; i.e.,  $\chi_i$ 's,  $\phi$ ,  $\psi$ ,  $\omega$ , and  $\Delta z$  were maintained fixed at the values in Table VII as  $z_{rot}$  varies. The computed values of  $[F_{rw}]_{rot}$  as a function of  $a$  ( $= b$ ) are shown in Figure 11. It seems that, while the minimum becomes deeper (indicating increased stabilization from this rotational entropy), it occurs at the same value of  $a$  ( $= b$ ) as the minimum in  $E_{total}$ . In this case, this entropy contribution is not enough to bring the minimum from 21.6 Å to the observed 23.3 Å; presumably, other entropy contributions (or possibly some effect of temperature on the energy parameters) would be required to achieve this agreement.

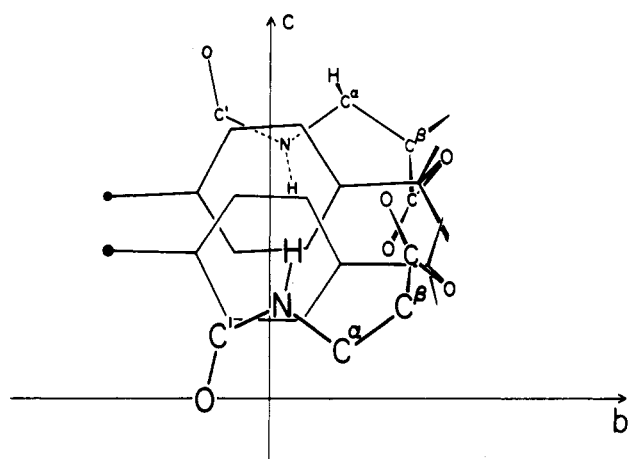


**Figure 13.** A  $b'-c$  projection of two packed antiparallel  $Rt(\omega)$  chains of  $\omega$ -helical  $p$ -Cl-PBLA in the minimum-energy conformation at  $a = b = 21.6$  Å of Table VII, showing the arrangement of the side chains and overlapping packing. The  $a'$  and  $b'$  axes are obtained by rotating the  $a$  and  $b$  axes by  $45^\circ$  counterclockwise about the  $c$  axis. For clarity, only one residue in each chain is shown. The chlorine atoms are indicated by solid circles.

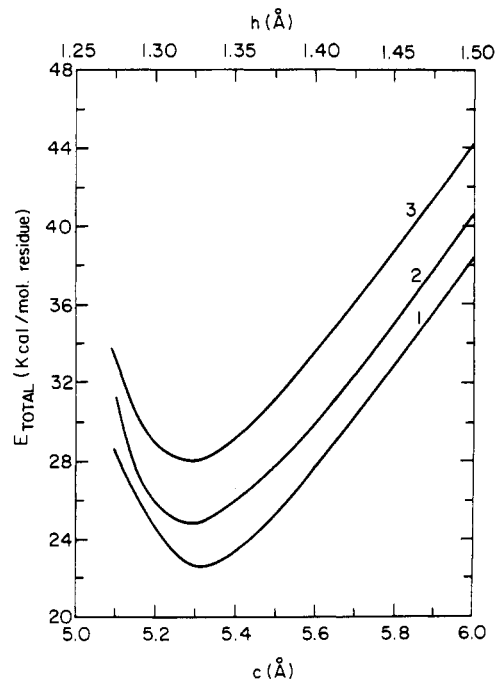


**Figure 14.** Dependence of  $E_{total}$  on  $c$  (and  $h$ ) for structure  $Rt(\omega)$  of  $\omega$ -helical  $p$ -Cl-PBLA for the following values of the lattice constants  $a$  ( $= b$ ): (1) 21.6 Å; (2) 23.3 Å; and (3) isolated  $\omega$ -helix. The parameters  $\omega$  and  $t$  were held fixed at  $-175.5$  and  $90^\circ$ , respectively.  $E_{total}$  was minimized with respect to the  $\chi_i$ 's,  $\Delta z$ , and  $z_{rot}$  at each value of  $c$  (and  $h$ ).

Taking  $\Delta F$  as  $[F_{rw} - F_{r\alpha}]_{rot}$  at a given temperature,<sup>35</sup> the values of  $\Delta F$  are 1.29 and 1.07 kcal per mol of residue at 300°K and 463°K, respectively, where  $F_{rw}$  is computed at  $a = b = 21.6$  Å and  $F_{r\alpha}$  at  $a = b = 13.75$  Å; these values of  $F_{rw}$  and  $F_{r\alpha}$  are those of minimum free energy. Thus, the  $\omega$  helix becomes more stable with respect to the  $\alpha$ -helix at 463°K than it is at 300°K. However, if the  $\omega$  helix is indeed a thermodynamically stable form at 463°K, then  $\Delta F$  should be negative at the higher temperature. Conceivably, this disagreement, as well as that between the computed and observed values of  $a$  ( $= b$ ), might be resolved if an additional entropy contribution<sup>56</sup> (from librational motions of the side chains) or temperature-de-

pendent energy parameters were included in the computations.

The distance between the chlorine atoms and the axis of the  $\omega$  helix was computed as 6.7 and 7.3 Å at  $a (= b) = 21.6$  and 23.3 Å, respectively, which is larger than those found for the  $\alpha$  helix (see Table V). The computed orientations of the transition moments of the various vibrations are also shown in Table V, but we are unaware of any experimental data with which these may be compared.

An  $a - b$  projection of one complete turn of the minimum-energy packed  $\omega$ -helical structure, showing the orientations of adjacent *p*-chlorobenzyl groups, is given in Figure 12. The alignment of these polar side chains shows that the dipoles would be parallel and, hence, result in repulsive intermolecular electrostatic interactions. However, as shown in Table VI, such an alignment also results in very attractive nonbonded interactions. In Figure 13, the favorable stacking of the phenyl groups of adjacent molecules is illustrated; the distance between phenyl rings is 3.84 Å, which is closer than calculated in the  $\alpha$  helix, i.e., 4.2 Å. The Rt( $\omega$ ) crystal is stabilized by this intermolecular phenyl...phenyl nonbonded attractive interaction.

In a final calculation on the  $\omega$ -helical structure, the restriction to a fixed backbone conformation was removed to determine how the crystal packing influences  $\phi$  and  $\psi$  (with  $\omega$  fixed at  $-175.5^\circ$  and  $t$  at  $90^\circ$  to retain the  $\omega$ -helical conformation). The values of  $E_{\text{total}}$  were minimized with respect to the  $\chi_i$ 's,  $\Delta z$  and  $z_{\text{rot}}$  at each value of  $h$  (and consequently  $c$ ) (i.e.,  $\phi$  and  $\psi$  for fixed  $\omega$ ) for the isolated homopolymer and for two selected values of  $a (= b)$ , viz., 21.6 and 23.3 Å. The results, plotted as  $E_{\text{total}}$  vs.  $h$  (or  $c$ ) in Figure 14 for the isolated homopolymer and for two values of  $a (= b)$ , show that the minimum-energy conformation occurs at the same value of  $h$  (or  $c$ ) for the isolated homopolymer and for both sets of values of  $a (= b)$ , viz., at 5.3 Å (or  $h = 1.33$  Å), in very good agreement with the experimental value<sup>6</sup> of 5.2 Å.

## Conclusions

In the crystal packing of  $\alpha$ -helical *p*-Cl-PBLA, it has been shown that structure Rt(–) of Yan *et al.*<sup>26</sup> is energetically much more stable than structure T(R) of Takeda *et al.*<sup>6</sup> The computed values of  $r_{\text{Cl}}$  and the orientations of the transition moments with respect to the helix axis are in reasonable agreement with the experimental results. These imply further that structure Rt(–) is likely the most probable structure in the crystal of  $\alpha$ -helical *p*-Cl-PBLA, although the backbone conformation may be slightly distorted from that of an ideal  $\alpha$  helix, as was observed<sup>30</sup> for PBLA.

The computations on the crystal packing of  $\omega$ -helical *p*-Cl-PBLA lead to several interesting conclusions. First, the energy calculations support the existence of the  $\omega$  helix in the crystal, as had been found from the X-ray diffraction studies.<sup>6</sup> Second, from Table VI, we expect that the direction of the transition moments of the  $\omega$  helix do not differ much from those of the  $\alpha$  helix; however, we would expect that  $r_{\text{Cl}}$  of the  $\omega$  helix would be larger than that of the  $\alpha$  helix. Third, the distance between two neighboring  $\omega$ -helix chains at  $a = b = 21.6$  Å was found to be 15.27 Å which is longer than 13.5 Å which we found for the  $\alpha$  helix at its most stable conformation. This fact, plus the result that  $\Delta F$  decreases at high temperature, implies that in order to transform the stable  $\alpha$  helix at room temperature to the stable  $\omega$  helix, an increase of temperature is necessary.

**Acknowledgment.** We are indebted to Drs. A. W. Burgess, F. A. Momany, L. L. Shipman, and S. Tanaka for

helpful discussion and to Mrs. Shirley Rumsey for assistance with these calculations.

## References and Notes

- (1) This work was supported by research grants from the National Science Foundation (GB-28469X3), from the National Institute of General Medical Sciences of the National Institutes of Health, U. S. Public Health Service (GM-14312), from the Eli Lilly Grants Committee, and from Walter and George Todd.
- (2) (a) N.I.H. Postdoctoral Trainee, 1971; Postdoctoral Fellow of the National Institute of General Medical Sciences, National Institutes of Health, 1971–1973. (b) N.I.H. Postdoctoral Trainee, 1968–1969; Postdoctoral Fellow of the National Institute of General Medical Sciences, National Institutes of Health, 1969–1971. Worcester Foundation for Experimental Biology, Shrewsbury, Mass. 01545.
- (3) R. F. McGuire, G. Vanderkooi, F. A. Momany, R. T. Ingwall, G. M. Crippen, N. Lotan, R. W. Tuttle, K. L. Kashuba, and H. A. Scheraga, *Macromolecules*, **4**, 112 (1971).
- (4) R. F. McGuire, F. A. Momany, and H. A. Scheraga, *J. Phys. Chem.*, **76**, 375 (1972).
- (5) F. A. Momany, L. M. Carruthers, R. F. McGuire, and H. A. Scheraga, *J. Phys. Chem.*, **78**, 1595 (1974). Data are reported by P. N. Lewis, F. A. Momany and H. A. Scheraga, *Isr. J. Chem.*, **11**, 121 (1973).
- (6) Y. Takeda, Y. Iitaka, and M. Tsuboi, *J. Mol. Biol.*, **51**, 101 (1970).
- (7) E. M. Bradbury, A. R. Downie, A. Elliott, and W. E. Hanby, *Proc. Roy. Soc., Ser. A*, **259**, 110 (1960).
- (8) R. H. Karlson, K. S. Norland, G. D. Fasman, and E. R. Blout, *J. Amer. Chem. Soc.*, **82**, 2268 (1960).
- (9) M. Goodman, C. M. Deber, and A. M. Felix, *J. Amer. Chem. Soc.*, **84**, 3771 (1962).
- (10) M. Tsuboi, *J. Polym. Sci.*, **59**, 139 (1962).
- (11) M. Goodman, A. M. Felix, C. M. Deber, A. R. Brause, and G. Schwartz, *Biopolymers*, **1**, 371 (1963).
- (12) M. Goodman, F. Boardman, and L. Listowsky, *J. Amer. Chem. Soc.*, **85**, 2491 (1963).
- (13) D. F. Bradley, M. Goodman, A. M. Felix, and R. Records, *Biopolymers*, **4**, 607 (1966).
- (14) M. Hashimoto and J. Aritomi, *Bull. Chem. Soc. Jap.*, **39**, 2707 (1966).
- (15) M. Hashimoto, *Bull. Chem. Soc. Jap.*, **39**, 2713 (1966).
- (16) M. Hashimoto and S. Arakawa, *Bull. Chem. Soc. Jap.*, **40**, 1698 (1967).
- (17) E. M. Bradbury, B. G. Carpenter, and H. Goldman, *Biopolymers*, **6**, 837 (1968).
- (18) E. H. Erenrich, R. H. Andreatta, and H. A. Scheraga, *Biopolymers*, **7**, 805 (1969).
- (19) E. H. Erenrich, R. H. Andreatta, and H. A. Scheraga, *J. Amer. Chem. Soc.*, **92**, 1116 (1970).
- (20) J. M. Squire and A. Elliott, *J. Mol. Biol.*, **65**, 291 (1970).
- (21) H. Obata and H. Kanetsuna, *J. Polym. Sci.*, **9**, 1977 (1971).
- (22) E. T. Samulski and A. V. Tobolsky, *Biopolymers*, **10**, 1013 (1971).
- (23) E. M. Bradbury, B. G. Carpenter, and R. M. Stephens, *Macromolecules*, **5**, 8 (1972).
- (24) T. Ooi, R. A. Scott, G. Vanderkooi, and H. A. Scheraga, *J. Chem. Phys.*, **46**, 4410 (1967).
- (25) J. F. Yan, G. Vanderkooi, and H. A. Scheraga, *J. Chem. Phys.*, **49**, 2713 (1968).
- (26) J. F. Yan, F. A. Momany, and H. A. Scheraga, *J. Amer. Chem. Soc.*, **92**, 1109 (1970).
- (27) E. M. Bradbury, L. Brown, A. R. Downie, A. Elliott, W. E. Hanby, and T. R. R. McDonald, *Nature (London)*, **183**, 1736 (1959).
- (28) E. M. Bradbury, L. Brown, A. R. Downie, A. Elliott, R. D. B. Fraser, and W. E. Hanby, *J. Mol. Biol.*, **5**, 230 (1962).
- (29) Recently, Baldwin *et al.*<sup>30</sup> suggested that their electron diffraction data on poly( $\beta$ -benzyl-L-aspartate) could be interpreted by assuming that both the atomic coordinates of the polymer and the fourfold symmetry of a true  $P4_3$  crystal are distorted. Unfortunately, such a model cannot be tested easily by conformational energy calculations because of the large increase in the number of variables required to accommodate these distortions. Furthermore, since these distortions (if present) must be small in order to obtain a good crystal, we have retained our assumption of a fixed geometry and a perfect crystal lattice.
- (30) J. P. Baldwin, E. M. Bradbury, I. F. McLuckie, and R. M. Stephens, *Macromolecules*, **6**, 83 (1973).
- (31) IUPAC-IUB Convention, Commission on Biochemical Nomenclature, *Biochemistry*, **9**, 3471 (1970).
- (32) H. Sugeta and T. Miyazawa, *Biopolymers*, **5**, 673 (1967).
- (33) R. A. Scott, G. Vanderkooi, R. W. Tuttle, P. M. Shames, and H. A. Scheraga, *Proc. Nat. Acad. Sci. U. S. A.*, **58**, 2204 (1967).
- (34) H. A. Scheraga, *Advan. Phys. Org. Chem.*, **6**, 103 (1968).
- (35) N. Gö, M. Gö, and H. A. Scheraga, *Proc. Nat. Acad. Sci. U. S. A.*, **59**, 1030 (1968); M. Gö, N. Gö, and H. A. Scheraga, *J. Chem. Phys.*, **52**, 2060 (1970); *ibid.*, **54**, 4489 (1971).
- (36) R. A. Scott and H. A. Scheraga, *J. Chem. Phys.*, **45**, 2091 (1966).
- (37) L. Brown and I. F. Trotter, *Trans. Faraday Soc.*, **52**, 537 (1956).
- (38) A. R. Downie, A. Elliott, W. E. Hanby, and B. R. Malcolm, *Proc. Roy. Soc., Ser. A*, **242**, 325 (1957).
- (39) S. Arnott, S. D. Dover, and A. Elliott, *J. Mol. Biol.*, **30**, 201 (1967).

- (40) B. R. Malcolm, *Biopolymers*, **9**, 911 (1970).
- (41) F. Happey, D. W. Jones, and B. M. Watson, *Biopolymers*, **10**, 2039 (1971).
- (42) For the calculations of the rotational entropy contribution to the Helmholtz conformational free energy described here, the lattice constant  $c$ , which is in the direction of the helix axis, is assumed to be fixed at the observed crystallographic value.
- (43) The isolated  $\omega$  helix is not a minimum-energy backbone conformation. The minimization referred to here is one where the side-chain dihedral angles were allowed to vary, with the backbone conformation held fixed.
- (44) Even though 4 residues is only one turn of an  $\omega$  helix, the dihedral angles resulting from the computation with such a short helix were used only as starting values for a subsequent calculation on a crystalline array of  $\omega$  helices, in which 12 residues/chain were taken (see section C).
- (45) The starting conformation for the  $\omega$  helix was chosen in this manner because no other data were available, either from a complete theoretical study of the  $\omega$  helix or from an X-ray conformation of the  $\omega$  helix of *p*-Cl-PBLA.
- (46) Since we are comparing the energy *per residue*, this comparison is almost valid (and would become more so as the chain length increases) even though 18 and 4 residues are used in the computations for the  $\alpha$  and  $\omega$  helices, respectively.
- (47) The X-ray results were interpreted<sup>6</sup> in terms of a random distribution of up and down chains. This suggests that, during nucleation, both up and down arrangements are equally probable without any energetic preference for one or the other arrangement. For simplicity in studying the crystal packing, we have thus assumed that all helical chains run in the same direction.
- (48) Here,  $E_{\text{total}}$  refers to  $E_{\text{ip}}(a, b, |q_i^0|_{i \neq z_{\text{rot}}, z_{\text{rot}}})$  defined in eq 19.
- (49) The Helmholtz conformational free energy per residue was computed only for  $\text{Rt}(-)$  and not  $\text{T(R)}$ , since  $\text{Rt}(-)$  is the lower-energy structure. For each  $a (= b)$ ,  $E_{\text{intra}}$  is a constant since the backbone is the fixed  $\text{Rt}(-)$  conformation; hence, only  $E_{\text{inter}}$  varies with  $z_{\text{rot}}$  (Figure 7).
- (50) From infrared dichroism studies of fibers of poly(ethylene sebacate),<sup>51</sup> the transition moment of the  $\text{C=O}$  stretching vibrations is  $19^\circ$  away from the  $\text{C=O}$  bond (in the direction of the  $\text{C}^\beta\text{—C}^\gamma$  bond) and, from similar studies of crystalline dimethyl oxalate, the transition moment of the  $\text{C—O—C}$  antisymmetric stretching vibration lies in the  $\text{COO}$  plane and is nearly perpendicular to the  $\text{C=O}$  bonds.<sup>52,53</sup>
- (51) E. M. Bradbury, A. Elliott, and R. D. B. Fraser, *Trans. Faraday Soc.*, **56**, 1117 (1960).
- (52) J. K. Wilmschurst, *J. Mol. Spectrosc.*, **1**, 201 (1957).
- (53) T. Miyazawa and K. Kuratani, *Nippon Kagaku Zasshi*, **72**, 804 (1951).
- (54) Only selected values of  $a = b$  were considered because of limitations on computer time, and because it was our intent here to determine (i) if a minimum-energy conformation would occur with only a small distortion in the  $\alpha$  helix, and (ii) whether a distortion in the  $\alpha$ -helix conformation favored an expansion or contraction of the lattice.
- (55) Since no geometry has been presented for the  $\omega$  helix, we chose the values of  $\phi$ ,  $\psi$ , and  $\omega$  from our minimum-energy conformation<sup>43</sup> for the isolated chain (last line of Table II); these values of  $\phi$ ,  $\psi$ , and  $\omega$  reproduce the experimental values of  $h$  and  $t$ .
- (56) The volume *per residue* occupied by  $\text{Rt}(-)$  and  $\text{Rt}(\omega)$  crystals at their minimum-energy conformations are 215 and 238 Å<sup>3</sup>, respectively, calculated as  $\pi d^2 h / 4$ , where  $d$  is the distance between two neighboring helical chains (13.5 and 15.3 Å for  $\alpha$  and  $\omega$  helices, respectively). This may indicate that structure  $\text{Rt}(\omega)$  has more room for the side chains to move than has  $\text{Rt}(-)$ .

## Conformational Analysis of the 1,3,5,7-Tetramethylcyclooctane Stereoisomers

D. R. Ferro, F. Heatley, and A. Zambelli\*

*Istituto di Chimica delle Macromolecole del CNR, 20133 Milan, Italy, and the Department of Chemistry, University of Manchester, Manchester, M13 9PL, United Kingdom. Received December 4, 1973*

**ABSTRACT:** A theoretical conformational analysis of the four stereoisomers of 1,3,5,7-tetramethylcyclooctane has been carried out using Warshel and Lifson's consistent force field. Two nonequivalent stable conformers were found for the *mmrr* isomer, while in the case of the other isomers only equivalent conformers contribute significantly to the equilibrium population at room temperature; the energy paths connecting the minima were also examined. The results of the calculations show the failure of less refined methods, based on geometrical assumptions, in the study of sterically hindered systems. The nmr spectra of the four isomers were measured at 220 MHz in *o*-dichlorobenzene and successfully analyzed. The vicinal proton coupling constants are fairly well correlated with the values calculated from the theoretical conformations using various forms of the Karplus equation, thus supporting the structures elucidated by the energy calculations. On the other hand, there is no simple connection between chemical shifts and conformations or configurations; this result indicates that great caution should be used when correlating chemical shifts and conformations of complex and sterically strained systems.

Rotational isomeric state theory and related methodology have been used for relating molecular properties of polymers to their chemical structure.<sup>1</sup> Such methods however require more and more refined conformational energy evaluations as more detailed correlations are wanted.<sup>2</sup> Therefore it cannot be stated that the literature is lacking in controversies even with regard to such extensively studied and relatively simple polymers as isotactic polypropylene.<sup>2-10</sup> To a certain extent the disagreement may stem from the difficulty of describing a macromolecule precisely, from uncertainties in the determination of physical properties of polymers, and perhaps from the fact that different researchers have examined nonidentical polymers. A related relevant problem, given the importance of nmr spectroscopy as a tool for the configurational and conformational studies of polymers, is to establish to what extent not only the vicinal proton coupling constants, but also the chemical shifts can be reliably correlated to the conformeric populations.<sup>5,11</sup>

In order to clarify the last point, as well as to test the current theoretical methods of analysis, the four stereoisomers of 1,3,5,7-tetramethylcyclooctane (TMCO) have been synthesized as reported elsewhere.<sup>12</sup> For each of these compounds extensive conformational energy calculations have been performed and the results have been checked against the nmr spectra.

### Method of Calculation

In recent years the advent of large computers and the development of procedures for finding the minima of many-variable functions have made possible a considerable progress in the prediction of the structure and of other molecular properties of hydrocarbons. Several authors<sup>13-16</sup> have proposed similar methods, which have been verified against a wealth of experimental data; common to all these methods are the assumptions that the Born-Oppenheimer potential energy surface of a molecule can be empirically represented by a sum of terms and